JOURNAL OF PETROLOGY | VOLUME 46 | NUMBER 11 | PAGES 2313–2336 | 2005 | doi:10.1093/petrology/egi056

Similar V/Sc Systematics in MORB and Arc Basalts: Implications for the Oxygen Fugacities of their Mantle Source Regions

CIN-TY AEOLUS LEE[1]*, WILLIAM P. LEEMAN[1], DANTE CANIL[2] AND ZHENG-XUE A LI[1]

[1]DEPARTMENT OF EARTH SCIENCES, MS-126, RICE UNIVERSITY, 6100 MAIN STREET, HOUSTON, TX 77005, USA

[2]SCHOOL OF EARTH AND OCEAN SCIENCES, UNIVERSITY OF VICTORIA, PETCH BUILDING, ROOM 280, 3800 FINNERTY ROAD, VICTORIA, BC, CANADA V8W 3P6

RECEIVED JULY 15, 2004; ACCEPTED MAY 3, 2005
ADVANCE ACCESS PUBLICATION JUNE 13, 2005

V/Sc systematics in peridotites, mid-ocean ridge basalts and arc basalts are investigated to constrain the variation of fO_2 *in the asthenospheric mantle. V/Sc ratios are used here to 'see through' those processes that can modify barometric* fO_2 *determinations in mantle rocks and/or magmas: early fractional crystallization, degassing, crustal assimilation and mantle metasomatism. Melting models are combined here with a literature database on peridotites, arc lavas and mid-ocean ridge basalts, along with new, more precise data on peridotites and selected arc lavas. V/Sc ratios in primitive arc lavas from the Cascades magmatic arc are correlated with fluid-mobile elements (e.g. Ba and K), indicating that fluids may subtly influence* fO_2 *during melting. However, for the most part, the average V/Sc-inferred* fO_2*s of arc basalts, MORB and peridotites are remarkably similar (−1·25 to +0·5 log units from the FMQ buffer) and disagree with the observation that the barometric* fO_2*s of arc lavas are several orders of magnitude higher. These observations suggest that the upper part of the Earth's mantle may be strongly buffered in terms of* fO_2*. The higher barometric* fO_2*s of arc lavas and some arc-related xenoliths may be due respectively to magmatic differentiation processes and to exposure to large, time-integrated fluid fluxes incurred during the long-term stability of the lithospheric mantle.*

KEY WORDS: *vanadium; scandium; oxygen fugacity; mantle; arcs*

INTRODUCTION

The purpose of this study is to constrain the oxygen fugacity (fO_2) of the asthenosphere—that part of the upper mantle that is mobile enough to undergo adiabatic decompression and is the dominant source region for most juvenile magmas in arcs and in mid-ocean ridges. Oxygen fugacity is defined as the activity (or roughly the partial pressure) of O_2 within a system (Carmichael, 1991; Frost, 1991; Kress & Carmichael, 1991) and represents an intensive variable (such as pressure and temperature) that provides a measure of the system's redox potential at equilibrium. Our interest in fO_2 is motivated by the fact that fO_2 controls the valence state, and hence speciation, of redox-sensitive elements. For example, fO_2 controls the mobility of redox-sensitive trace metals (e.g. first series transition metals and the platinum group elements) and the species composition of volcanic gases emitted to the ocean–atmosphere system. Understanding how fO_2 varies in space and time therefore has important implications for studies of ore genesis, atmospheric evolution and trace-element partitioning.

In practice, fO_2 is determined indirectly by O_2 thermobarometry wherein the activities of the different valence states of a redox-sensitive element in minerals and/or glasses are measured. In homogeneous (single phase) systems, e.g. a melt, experimentally calibrated relationships between fO_2 and the activities of Fe^{3+} and Fe^{2+} in a glass are typically used to obtain the fO_2 of a magma just prior to quenching (Christie *et al.*, 1986; Kress & Carmichael, 1991). In a heterogeneous (e.g. multiphase) system, the fO_2 of last equilibration is recorded by the distribution of Fe^{3+} in different system phases. For example, pertinent to peridotitic mantle lithologies,

*Corresponding author. Telephone: 1-713-348-5084. E-mail: ctlee@rice.edu

the reaction

$$6Fe_2SiO_{4(Ol)} + O_{2(fluid)} = 2Fe_3O_{4(Sp)} + 3Fe_2Si_2O_{6(Opx)} \quad (1)$$

where fayalite, magnetite and ferrosilite appear as components in solid solution with olivine, spinel and orthopyroxene, respectively (Mattioli & Wood, 1986; Wood & Virgo, 1989; Ballhaus *et al.*, 1990, 1991), provides an indirect measure of the fO_2 of a peridotite just before it cooled through its closure temperature. These methods for estimating the fO_2 of last equilibration are referred to here as 'barometric fO_2'.

The barometric method of inferring fO_2 has now been widely applied to mantle xenoliths and lavas. Mid-ocean ridge basalts (MORB) appear to have barometric fO_2s systematically lower than that of arc lavas: relative to the fayalite–magnetite–quartz (FMQ) buffer, MORB have fO_2s between −2 and 0 log units from the FMQ buffer (herein referred to as FMQ–2 and FMQ), whereas arc lavas have fO_2s ranging between FMQ and FMQ+6 (Christie *et al.*, 1986; Carmichael, 1991). If these magma fO_2s directly reflect that of their mantle source regions, it must be concluded that sub-arc mantle is more oxidized than ambient mantle. That sub-arc asthenosphere is oxidized is, arguably, a widely accepted view, and has led to the paradigm that oxidation of the mantle is related, in some manner, to the availability of oxidized fluids or sediments originating from the subducting slab (Carmichael, 1991). Possibilities include overprinting by hydrous fluids characterized by high fO_2 (Carmichael, 1991) and/or addition of silicic magmas derived from melting of hot subducting and oxidized oceanic crust (Mungall, 2002). The problem, however, is that true primary arc magmas are extremely rare. This begs the question of whether the fO_2s of arc magmas are really representative of their magma source regions. In fact, a number of magmatic differentiation processes can lead to oxidation of a magma. For example, early fractional crystallization of reduced minerals, interaction with oxidizing fluids or wall rock derived from continental crust, or degassing of reduced species of C, H and S (Mathez, 1984) may lead to an increase in fO_2. In addition, reaction of H_2O with reduced species (e.g. Fe^{2+}) in conjunction with preferential loss of H_2 to the atmosphere can result in auto-oxidation of the magma without any open-system exchange other than H_2 loss (Sato & Wright, 1996; Holloway, 2004). Given these possibilities for increasing oxidation, the range in barometric fO_2 of arc lavas is a maximum bound on their source regions, e.g. arc asthenosphere.

An alternative approach for determining the fO_2 of arc asthenospheric mantle is to study arc mantle xenoliths. Indeed, peridotite xenoliths from arc-related environments, such as those from Simcoe near the Washington Cascades, Japan, and the Solomon Islands (Brandon & Draper, 1996; Parkinson & Arculus, 1999), appear to record higher barometric fO_2s (up to FMQ+2), but these values still do not match the higher values seen in some arc lavas. Similarly, the majority of continental peridotite xenoliths, some of which may have originated in or been influenced by arc magmas or fluids, have barometric fO_2s ranging between FMQ–2 and FMQ+1 (Mattioli & Wood, 1986; Wood & Virgo, 1989; Ballhaus *et al.*, 1990, 1991), overlapping the barometric fO_2s of MORB, and lower than that of most arcs. Only the unusual amphibole-bearing mini-xenoliths from western Mexico record higher barometric fO_2s (up to FMQ+4; Blatter & Carmichael, 1998). If these arc-related mantle xenoliths represent the source regions of arc lavas, we are faced with the paradox that their fO_2s are just not as high as those of arc lavas. However, it is possible that barometric fO_2s of mantle xenoliths have nothing to do with the fO_2s of arc magma source regions. This is because nearly all peridotite xenoliths at present derive from the lithospheric mantle, even though at some point they were part of the asthenosphere, and have undergone some amount of partial melting (see Fig. 1). This is evidenced by the fact that the last equilibration temperatures and pressures of most mantle xenoliths are typically subsolidus. What this means is that, given the long-term stability of the lithospheric mantle (Jordan, 1975; Pearson *et al.*, 1995; Griffin *et al.*, 1999; Lee *et al.*, 2001*a*; O'Reilly *et al.*, 2001), its barometric fO_2 is not likely to retain any information about the fO_2 of the asthenospheric mantle from which the lithosphere was derived. For example, lithospheric fO_2 is subject to overprinting by subsequent metasomatic events. In fact, most metasomatizing processes are likely to be oxidizing (McGuire *et al.*, 1991; McCammon *et al.*, 2001). This suggests that even the barometric fO_2s of arc-related mantle xenoliths are likely to be maximum bounds on the fO_2 of the asthenospheric mantle from which they have originally derived.

We are left with the question of what is the true fO_2 of arc asthenosphere, i.e. the source region to arc lavas, given that barometric fO_2s of arc lavas and xenoliths are maximum estimates. This uncertainty stems from the fact that barometric fO_2 records only the last equilibrium state and hence bears no memory of past equilibrium states. Thus, it is impossible to estimate the fO_2 of the asthenosphere by applying barometric fO_2 determinations to magmas that have already left their source regions, or to mantle xenoliths that have already cooled below their solidus temperatures and experienced subsequent metasomatic overprinting. What is needed is a proxy for fO_2 that retains a memory of the original fO_2 conditions attending melting in the asthenosphere. This original fO_2 is referred to here as the primary mantle or primary magma fO_2 (compare

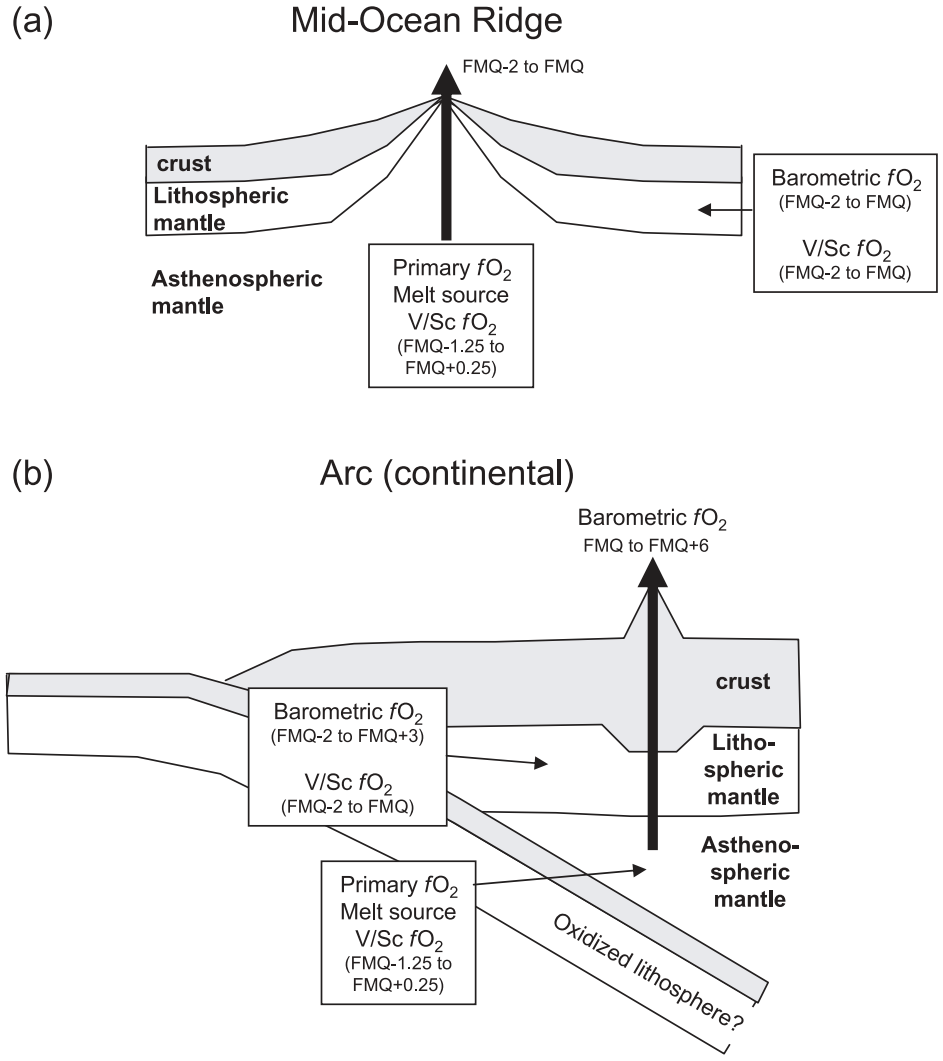

Fig. 1. (a) Schematic diagram showing the difference between barometric fO_2 and V/Sc-inferred fO_2 in a mid-ocean ridge system. (b) Similar diagram for an arc system. Barometric fO_2 in mantle xenoliths reflects the intrinsic fO_2 of the lithospheric mantle. Barometric fO_2 of lavas represents the intrinsic fO_2 of the magma. V/Sc-inferred fO_2 of peridotites and lavas reflects the fO_2 of asthenospheric mantle at the time of partial melting.

with the term primitive magma fO_2 to describe magmas that have experienced only minor amounts of differentiation since leaving their melt source regions). A requirement of this fO_2 proxy is that it must be able to 'see through' early differentiation processes in a magma and metasomatic processes in a mantle peridotite, allowing it to retain a memory of the original melting conditions.

Here, we develop the use of V/Sc ratio systematics in peridotites and magmas as a technique for retrieving primary fO_2. We choose V and Sc for the following reasons. The behaviors of V and Sc during mantle melting are more similar to each other than to any other elements, as evidenced by their similar enrichments (Fig. 2) in continental crust, arc magmas and MORB relative to primitive mantle (Sun & McDonough, 1989; McDonough & Sun, 1995; Rudnick & Fountain, 1995): they are both mildly incompatible during the formation of MORB and arc lavas, and they are not mobile in fluids. However, superimposed on their overall geochemical similarities is the fact that, in detail, the speciation and thus the partitioning of V is redox-sensitive, whereas that of Sc is not (Fig. 3). V concentrations of primitive melts and residual peridotites are predicted to depend on the fO_2 conditions attending melting (Canil & Fedortchouk, 2000; Canil, 2002). The use of V/Sc ratios rather than V alone helps to reduce the effects of magmatic differentiation processes that may dilute V

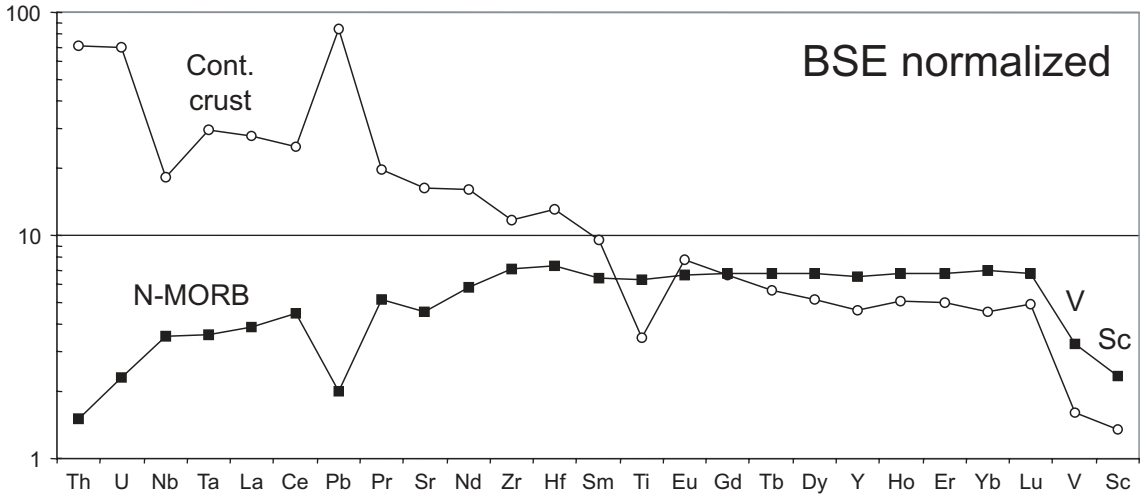

Fig. 2. Trace-element compositions of bulk continental crust (Cont. Crust) and average mid-ocean ridge basalt (N-MORB) normalized to Bulk Silicate Earth (BSE; McDonough & Sun, 1995). Elements are plotted in approximate order of increasing compatibility (Hofmann, 1988). Note the similar enrichments in V and Sc in both continental crust and N-MORB.

and Sc concentrations, but not significantly modify their relative proportions. This is because early fractional crystallization of olivine will not affect the V/Sc ratio of the magma, as both elements are highly incompatible in olivine. Finally, two additional properties of V and Sc make them ideal for constraining mantle fO_2 during melting: (1) in peridotites, these elements are not significantly affected by 'cryptic' metasomatism because they are only mildly incompatible (Canil, 2004), and (2) magmatic systems undergoing degassing remain closed to V and Sc exchange. Thus, V/Sc systematics in peridotites and primitive basalts may provide a simple but powerful tool for 'seeing through' processes of mantle metasomatism, magmatic degassing and early magmatic differentiation, allowing us to estimate the primary fO_2 during mantle melting.

THEORY: TRACKING MANTLE fO_2 USING V/Sc SYSTEMATICS

In this section, we develop the basis for using V/Sc systematics in residual peridotites and primitive lavas. We define residual peridotites as those having experienced melt extraction. We ignore those that represent cumulates or have significant melt–rock reaction products. Residual peridotites examined here have Mg-numbers [molar Mg/(Mg + Fe)] $\geq$ 0·88 and Al_2O_3 contents $\leq$4·3 wt %. Primitive lavas are defined here as those magmas that have experienced only minimal amounts of fractional crystallization. We thus consider only basaltic lavas having SiO_2 contents $<$ 52 wt % and MgO contents $>$ 6 wt % to be primitive. Such magmas are likely to have crystallized only olivine and minor amounts of spinel and clinopyroxene.

Modelling the fO_2 dependence of V/Sc during melting

Melting model

To illustrate the fO_2 dependence of V/Sc on partial melting, we begin with the following simplifying assumptions.

(1) Partial melting takes place at isothermal (1410°C) and isobaric (1·5 GPa) conditions, hence, the effects of changing pressure and temperature on mineral partition coefficients and melting stoichiometry are ignored.

(2) MORB and arc basalts largely originate from the spinel stability field, so we adopt the melting stoichiometry of fertile spinel peridotite (olivine + orthopyroxene + clinopyroxene + spinel) at 1·5 GPa, as determined using the pMELTS thermodynamic algorithm (Ghiorso *et al.*, 2002) and used by Lee *et al.* (2003).

(3) The V/Sc ratio of fertile convecting mantle is uniform.

Assumption (1) has been made because the exact P–T paths during decompressional melting beneath mid-ocean ridges and in the arc mantle wedge are not known. The errors introduced with this assumption are unlikely to be serious because the pressure dependence of V and Sc partitioning is small, and the range of temperature over which partial melting takes place is not very large (<200°C). Assumption (2) should not lead to large errors. The lack of strong garnet signatures in MORB and most arc basalts indicates that melting in the garnet stability field, although it does occur, is probably small. Nevertheless, in a later section, we will address the effects of garnet melting.

To model magma compositions, we assume that the erupted magmas represent aggregates of fractional melts and hence model the magmas as batch melts. The residual peridotite, on the other hand, is modelled as a

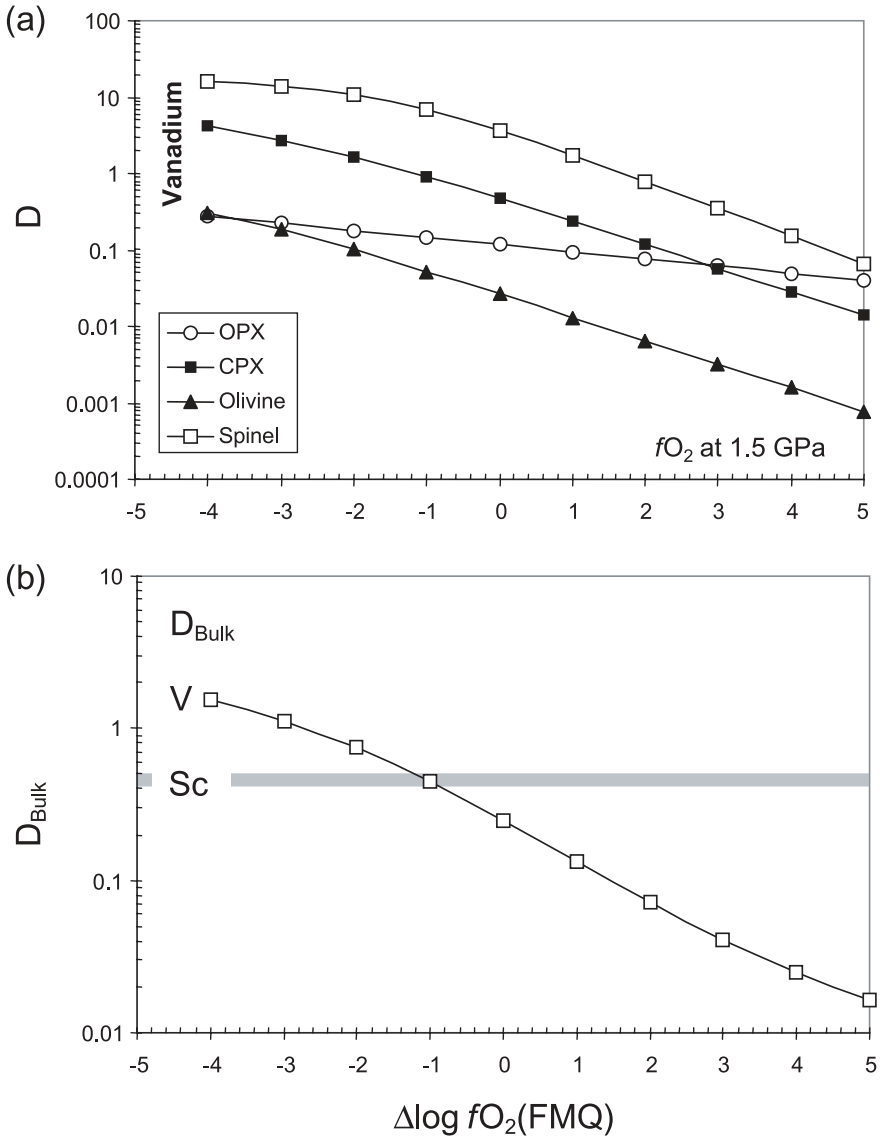

Fig. 3. (a) Vanadium partition coefficients for clinopyroxene, orthopyroxene, olivine, and spinel as a function of log fO_2 deviations (ΔFMQ) from the fayalite–magnetite–quartz buffer (FMQ); these partition coefficients use the parameterizations given by Canil (2002), but the ΔNNO (log unit deviation from the Ni–NiO buffer) units used by Canil have been converted to ΔFMQ units for conditions of 1·5 GPa, where the difference between the FMQ and NNO buffers is small. (b) Bulk V and Sc partition coefficients for a spinel lherzolite.

fractional residue by assuming incremental extraction of small-degree batch melts. We used the pMELTS thermodynamic algorithm (Ghiorso *et al.*, 2002) to model the melting stoichiometry at 1·5 GPa (Lee *et al.*, 2003).

Initial V and Sc concentrations in the source

The initial V and Sc concentrations (V_o and Sc_o) of the mantle prior to melt extraction are assumed to be equivalent to that of 'primitive mantle', also known as 'bulk silicate Earth' (BSE). These values were determined as follows. Sc_o was estimated by multiplying the estimated Al content of BSE by the chondritic Sc/Al ratio under the assumption that Sc and Al are both refractory lithophile elements and therefore should remain in chondritic proportions in the BSE. This yields Sc_o of 16·5 ppm (McDonough & Sun, 1995). Unlike Sc and Al, V is moderately volatile and moderately siderophile; hence, some fraction may have been volatilized or lost to the core. Because V cannot be directly inferred from chondrites, we estimate V_o by considering peridotite melt depletion trends where V/Sc is plotted against MgO, Al_2O_3 and Sc, all of whose BSE concentrations have been previously estimated (Fig. 4; McDonough & Sun, 1995). Extrapolations based on an internally consistent database, which will be discussed below, result in a V_o/Sc_o of 4·9 (Fig. 4). This yields a V_o of 83 ppm

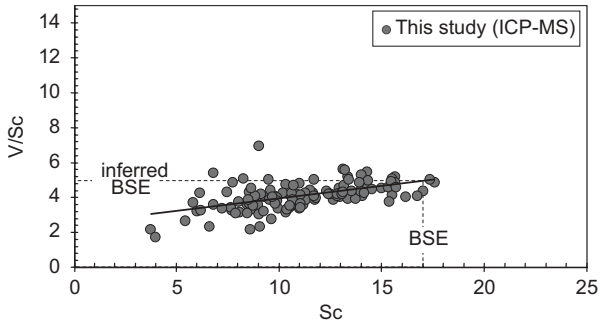

Fig. 4. V/Sc versus Sc (this study) for mantle xenoliths and obducted ophiolite peridotites. Sample localities are given in the Appendix. BSE refers to 'Bulk Silicate Earth'. Estimates of BSE Sc are from McDonough & Sun (1995). BSE V/Sc is determined from the intersection of the regression line with BSE Sc.

[compare $V_o \sim 82$ from McDonough & Sun (1995)]. We note that the mantle today is clearly not 'primitive' because it already has seen extraction of highly incompatible elements by the formation of continental crust. However, the net effect of the continental crust formation on major elements and moderately incompatible elements in the residual mantle is nearly negligible because continental crust makes up only 0·6% of the total mass of the BSE. Thus, for all intents and purposes, the V and Sc concentrations of the so-called 'depleted upper mantle' are considered here to be nearly identical to that of BSE models. We will return to the issue of mantle heterogeneities in the Discussion section.

Partition coefficients

We used the following partition coefficients for V and Sc (see Fig. 3). Parametrizations of V partitioning (D_V) for olivine, orthopyroxene, clinopyroxene and spinel as a function of fO_2 were summarized by Canil (2002). Experiments performed on spinels having different Cr-number [Cr/(Cr + Al)] indicate that for a given fO_2, V is more compatible in spinels with higher Cr content. The Cr-number of spinels increases with increasing melting degree. The effects are most pronounced at high degrees of melting (>20%) when Cr-numbers approach 0·7 as compared with 0·3 in peridotites having more fertile major element compositions. Some arc magmas probably represent higher-degree melts (or derive from more refractory sources) than MORB (Smith & Leeman, 2005), which makes it difficult to compare directly the V/Sc compositions of primitive MORB and arc lavas if they form by different degrees of melting. However, many arc lavas and MORB overlap in Cr/Al–MgO and TiO_2–MgO systematics (Fig. 5), suggesting that the majority of primitive arc lavas and MORB derive from similar degrees of melting. We thus use the same partition coefficients for spinel in our treatment of MORB and arc lavas. Temperature effects on V partitioning were not considered here, as Canil showed that the effects of variable fO_2 were much greater than the effects of temperature.

For Sc, we used published empirical parameterizations of D_{Sc} with respect to D_{MgO} for olivine and orthopyroxene (Beattie *et al.*, 1991; Jones, 1995), where D_{MgO} was constrained by the temperature at which melting was assumed to occur in our models (1410°C; Sugawara, 2000). For clinopyroxene, we used a D_{Sc} of 1·2, which represents the average of partition coefficients measured at 1380, 1405 and 1430°C (Hart & Dunn, 1993; Hauri *et al.*, 1994). The partitioning behavior of Sc in spinel is poorly known, but it is likely that Sc is highly incompatible in spinel. We thus assumed that $D_{Sc} \sim 0$ for spinel. We note that the low modal abundance of spinel, and its very low Sc partition coefficient, make the predicted Sc concentrations in the magma and solid residue insensitive to large uncertainties in the partition coefficient.

Application to melts and melt residues

In Fig. 6a, V/Sc ratios of 1·5 GPa melts are plotted as a function of F at given constant fO_2s. It can be seen that fO_2 and the degree of melting (F) both control the V/Sc in the melt. At low fO_2, V is more compatible than Sc, so the V/Sc ratio of the melt is low. At high fO_2, V becomes more incompatible than Sc, leading to high V/Sc ratios in the melt. The separations between V/Sc–fO_2 melting contours are greatest at low F but the contours converge at very high F due to mass balance effects. Strictly speaking, the fO_2 of the melt source region of primitive lavas can only be derived if the degree of melting required to produce the lava is known. However, it can be seen from Fig. 6a that V/Sc ratios are not very sensitive to F at intermediate degrees of melting ($F \sim 10\%$).

It is generally agreed that MORB represents aggregate melt fractions of ~10% based on relative enrichments of highly incompatible elements in MORB (Hofmann, 1988; Langmuir *et al.*, 1992). The average melting degree required to produce primitive arc lavas is more difficult to constrain by this approach because their source composition may be variably metasomatized by the passage of fluids. A more robust approach is to use Ti concentrations. Ti is a moderately incompatible element. Its abundance in a primitive magma, including primitive arc lavas, can be used as a qualitative inverse indicator of F because it is fluid-immobile, and hence its concentrations in the arc source are minimally affected by fluid metasomatism. Using this approach, tholeiitic-type arc lavas have been estimated to represent 6–10 wt % melts of fertile (in the major-element sense) spinel lherzolite (Baker *et al.*, 1994; Bacon *et al.*, 1997; Grove *et al.*, 2002), and are thus similar to MORB. In Fig. 5b, we compare MgO and TiO_2 for global arc lavas and MORB. We can see that MORB and primitive arc basalts (MgO > 8 wt %) have very similar

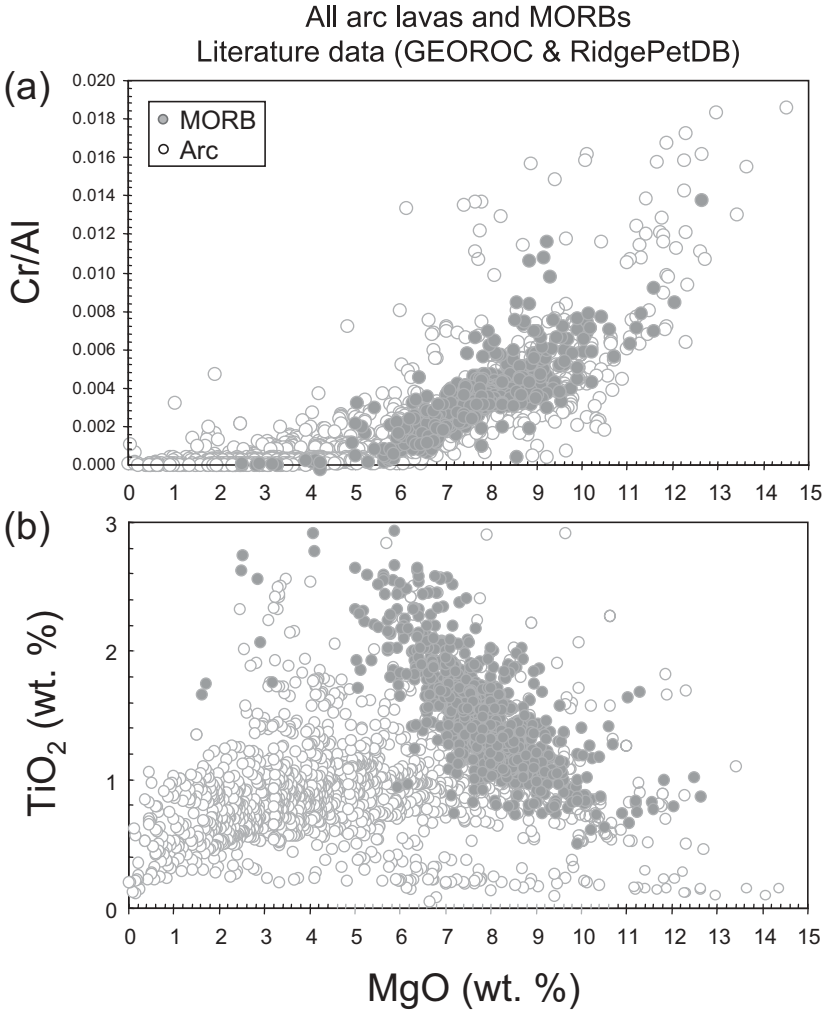

Fig. 5. (a) Cr/Al versus MgO (wt %) for arc lavas and MORB using global literature datasets (GEOROC and RidgePetDB). (b) TiO_2 (wt %) versus MgO (wt %) for arc lavas and MORB using the global literature dataset.

TiO_2 contents. Only a few arc basalts have lower TiO_2 contents, which would indicate higher degrees of melting or partial melting of a refractory source. For these reasons, we assume in all ensuing discussions that primitive arc lavas and MORB generally originate from 10% melting.

In the above modelling, the assumption is that partial melting takes place at constant fO_2, although there is no obvious reason why this should be the case. Constant fO_2 melting means that either the system is open to O_2 exchange and controlled by an external buffer, or that the change in phase proportions and distribution of Fe^{3+} and Fe^{2+} among the phases is such that constant fO_2 is fortuitously maintained. We assume constant fO_2 only because we do not know how to predict exactly how fO_2 varies during partial melting. It is often pointed out that because Fe^{3+} is more incompatible than Fe^{2+}, the bulk Fe^{3+} content of the residual mantle should decrease. This statement is often casually used to argue that the fO_2 of the residual mantle must decrease with progressive melt extraction. Although the first statement is indeed true, the latter statement is not only an over-simplification, but also represents a misunderstanding of what governs fO_2. Unlike a magma, which can be considered a homogeneous system, peridotites are heterogeneous systems and therefore the fO_2 of a peridotite is not recorded by the bulk Fe^{3+}/Fe^{2+} ratio, but rather by the proportioning of Fe^{3+} among the different system phases. As spinel is the dominant phase that incorporates Fe^{3+}, it is important to note that in a peridotite system assumed to be closed to O_2 exchange, the fO_2 of this system will be controlled largely by the activity of Fe^{3+} in spinel, which itself must be controlled by the modal proportion of spinel, because spinel is the only phase that takes in appreciable amounts of Fe^{3+}. Thus, if the spinel mode decreases, as it does during partial melting, the effect of decreasing bulk Fe^{3+} contents is counteracted by the concentrating of Fe^{3+} into smaller amounts of spinel. The end result is that the change in mantle fO_2 during

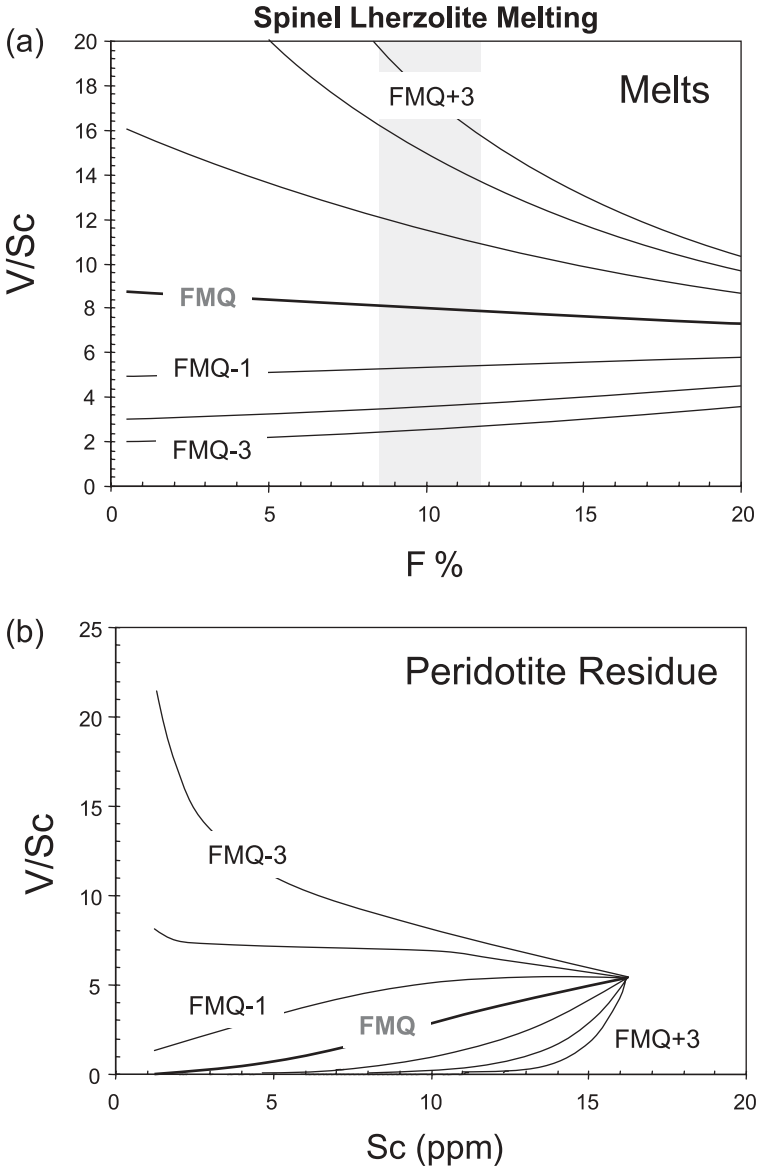

Fig. 6. (a) V/Sc ratio in primary melts as a function of degree of melting, *F*, in wt %, at given fO_2s. (b) V/Sc ratio versus Sc in residual peridotite calculated assuming fractional melt extraction at given fO_2s. Isopleths of fO_2 are denoted using Δlog unit deviations from the fayalite–magnetite–quartz buffer (FMQ), e.g. an fO_2 of FMQ–1 represents −1 log unit deviation from FMQ.

melting may be small. Consistent with this reasoning is the fact that the V systematics of peridotites have previously been shown to follow near constant fO_2 melting paths (Canil, 2002; Lee *et al.*, 2003). In any case, the fO_2 isopleths shown in our model results can be used to qualitatively assess the effect of changing fO_2 during melting.

Effects of fractional crystallization

In the above modelling, we have assumed from the outset that early fractional crystallization of olivine will not affect V/Sc ratios because D_V and D_{Sc} in olivine are very small [e.g. the exponent in the fractional crystallization equation $(V_m/Sc_m)/(V_m/Sc_m)_0 = F^{(D_{ol}^V - D^{Sc})}$ is nearly zero; where the subscript m denotes the melt and the subscript 0 denotes the original melt composition]. The effects of olivine fractionation are illustrated in Fig. 7a, where it can be seen that even over six orders of magnitude in fO_2, the effect of olivine crystallization on the magma V/Sc ratio is negligible. We can also consider the effects of spinel co-crystallization with olivine. V is compatible in spinel under most relevant fO_2 conditions, whereas Sc is incompatible (Fig. 3). As a consequence, significant spinel fractionation will result in a decrease in V/Sc ratio of the magma. In Fig. 7b and c, we show the effects of co-crystallizing spinel and olivine for the case in

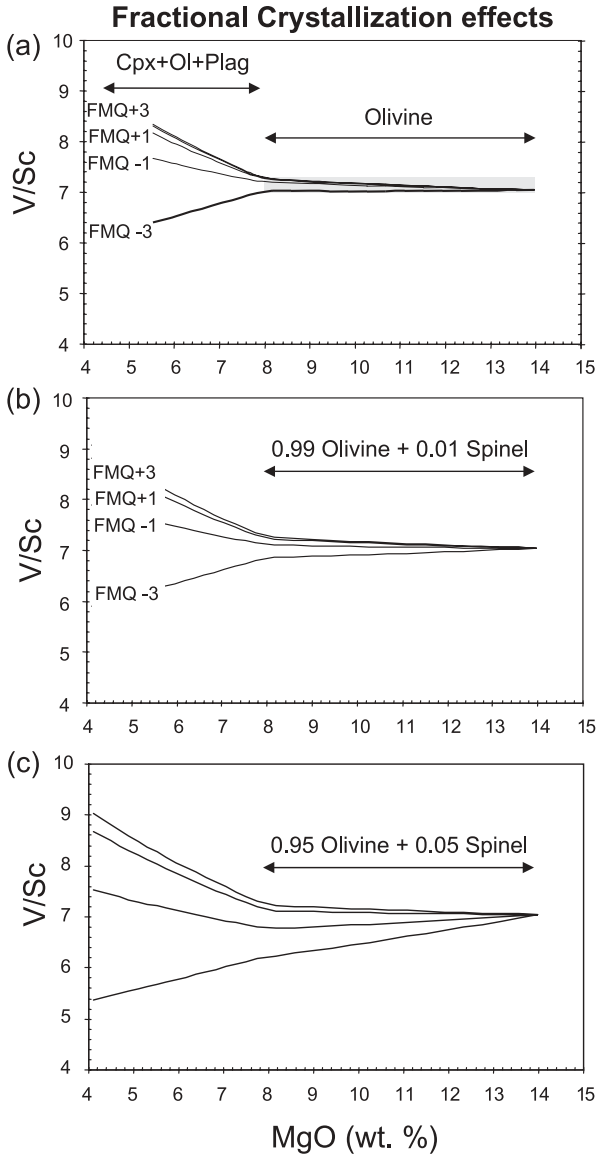

Fig. 7. The effects of fractional crystallization: (a) olivine crystallization between 14 and 8 wt % MgO; (b) olivine–spinel co-crystallization between 8 and 14 wt % MgO, where spinel makes up 1% of crystallizing phases; (c) same as in (b) except that spinel makes up 5% of crystallizing phases. At MgO < 8 wt %, co-crystallization of clinopyroxene (60%) and olivine (40%) is assumed for (a)–(c). Plagioclase crystallization does not have any effect on V, Sc or MgO due to the low contents of these elements in plagioclase.

which the proportion of spinel in the crystallizing solids is 1 and 5%. It can be seen that for these small amounts of spinel crystallization, the effect on V/Sc in the magma is actually fairly small relative to the large differences predicted in V/Sc at differing fO_2s. We note that although the total amount of spinel crystallization in basaltic magmas is difficult to constrain accurately, it is probably less than 5% based on petrographic observations. We thus conclude that for primitive magmas in which only

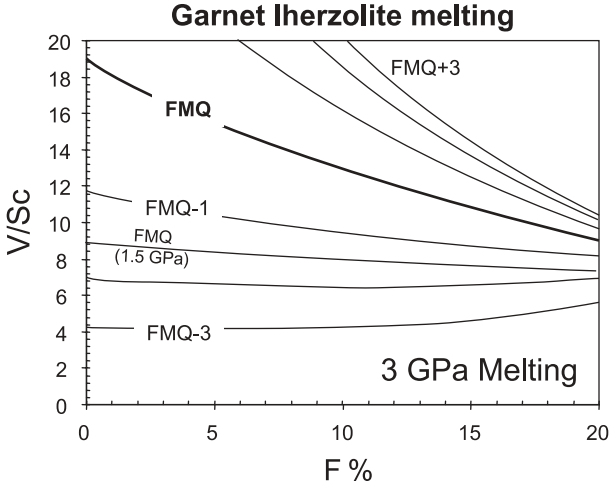

Fig. 8. The effects of melting in the garnet lherzolite field. Melting is assumed to take place at 3 GPa in this model using the melting stoichiometry of Walter (1998). Dashed line represents the FMQ melting isopleth at 1·5 GPa (spinel stability field). The effect of garnet is to increase the V/Sc ratio in the melt.

olivine and spinel are on the liquidus, the effects of fractional crystallization on V/Sc ratios can be largely ignored, and hence the measured V/Sc may be taken as representative of the primary V/Sc ratio.

On the other hand, we note that if clinopyroxene is on the liquidus, the effect on the V/Sc ratio of the magma may be large, particularly at higher fO_2s. This can be seen in Fig. 7a–c, where we have co-crystallized clinopyroxene and olivine at MgO < 8 wt %. Crystallization of clinopyroxene at fO_2s near FMQ or higher result in an increase in V/Sc in the melt. We also note that clinopyroxene crystallization results in a decrease in Sc concentration ($D_{Sc}^{cpx} > 1$), which is not typically seen in MORB and arc basalts with MgO contents greater than ~8 wt % MgO.

Effect of garnet during melting

Although melting in the garnet stability field is probably minor for MORB and most arc basalts, we can nevertheless address the role of garnet. Canil has shown that D_V for garnet under most terrestrial fO_2 conditions is likely to be less than one (Canil, 2002, 2004). Because D_{Sc} for garnet in basaltic systems is ~2·6 (Hauri *et al.*, 1994), melting of garnet lherzolites yields higher V/Sc than melts of spinel lherzolites for a given fO_2. In Fig. 8, we have explicitly modelled melting of lherzolite in the garnet stability field using experimentally determined melting stoichiometries at 3 GPa (Walter, 1998).

LITERATURE DATASETS AND INTERNALLY CONSISTENT DATA

The development of comprehensive geochemical databases (e.g. GEOROC and RidgePetDB) has provided an

unparalleled opportunity to investigate global geochemical correlations that might otherwise go unnoticed with small regional datasets. However, certain precautions must be considered when using literature compilations. V and Sc concentrations reported in the literature are often determined using different analytical techniques (XRF, ICP-MS, ICP-AES, INAA) and external standards. Thus, literature compilations may have an inherent level of uncertainty associated with inter-laboratory biases, as previously discussed by Lee *et al.* (2003). Theoretically, these biases can be corrected for but, unfortunately, this is seldom possible because the normalization values of external standards are not always published.

We can quantify how much of the scatter in the literature database is due to inter-laboratory bias by comparing the literature data with an internally consistent dataset for peridotites collected from different localities and tectonic settings. New V and Sc data were determined by inductively coupled plasma mass spectrometry using the USGS basalt standard BHVO-1 as an external standard. Normalization values for V and Sc in BHVO-1 are from Eggins *et al.* (1997). The peridotites analyzed include spinel peridotite xenoliths from various localities in western North America [Simcoe in the Washington Cascades (Brandon & Draper, 1996), Dish Hill and Cima in California, Vulcan's Throne in Arizona, Lunar Crater in Nevada, Kilbourne Hole in New Mexico], ophiolitic terranes in the western Sierra Nevada foothills (Feather River Ophiolite) and ophiolites and orogenic massifs in the North American Cordillera in British Columbia, Yukon and Alaska. The Simcoe xenoliths are believed to be related to arc mantle and have previously been shown to have barometric fO_2s up to FMQ+1·8 (Brandon & Draper, 1996). More details of our samples are presented in the Appendix.

The new V/Sc and Sc data are shown in Fig. 9a compared with the literature database of spinel peridotites. The literature data were not filtered for data quality and, hence, may not be internally consistent due to inter-laboratory bias. It can be seen that the literature V/Sc data are highly scattered. However, considering only the new, internally consistent peridotite data, there is much less scatter and there appears to be a subtle positive correlation between V/Sc and Sc, which is completely obscured using unfiltered literature data. The reduced scatter in the new dataset is remarkable, given that the chosen peridotites come from different localities and tectonic settings, and have different metasomatic histories. This supports the suggestion that the scatter seen in the literature database is probably due to inter-laboratory bias. It follows that the development of internally consistent V and Sc databases can potentially reveal additional structure in V/Sc systematics that may otherwise go unnoticed when using literature compilations.

Our discussion below is based on a combination of new data and literature-compiled data. Inter-laboratory bias and analytical uncertainties are likely to be largest for peridotites because their V and Sc contents often approach the detection limits of various analytical techniques (e.g. XRF). Thus, for peridotites, our interpretations are based only on new high-precision ICP-MS data. For MORB and arc lavas, analytical uncertainties are likely to be less problematic. Our discussion on lavas begins with the literature dataset for which there is an abundance of data. We then present a subset of V and Sc data for arc lavas, which we have independently confirmed (see the Appendix). In all ensuing discussion, we explicitly denote when new data (this study) and literature data are used.

CASE STUDIES

Peridotites (this study)

In Fig. 9b, we combine our model predictions with the new peridotite V and Sc data. These data represent a range of tectonic environments, including continental lithospheric mantle xenoliths from western North America, an orogenic massif and obducted ophiolites. There is a slight correlation between V/Sc and Sc. The range in Sc (from low values of ~5 up to values of ~17) reflects progressive depletion in Sc during melt extraction. The decrease in V/Sc with degree of melt extraction indicates that overall V is slightly more incompatible than Sc. When compared with the model predictions, most of the V/Sc–Sc data appear to closely follow the FMQ–1 melting curve; the total variation in fO_2 seems to be less than ±0·5 log units. The V/Sc-predicted fO_2s fall within the range of barometric fO_2 recorded for abyssal peridotites and MORB glasses (Christie *et al.*, 1986; Wood & Virgo, 1989; Wood *et al.*, 1990). These peridotites come from oceanic, arc and continental settings where barometric fO_2s in lavas range from −2 to +6 log units from the FMQ buffer. Considering the sensitivity of V/Sc ratio to fO_2, the uniformity in V/Sc (and, by inference, primary mantle fO_2) is remarkable.

MORB (RidgePetDB)

Here, we examine MORB data from the RidgePetDB database (Lehnert *et al.*, 2000). The MORB data comprise whole-rock and glass analyses from the Mid-Atlantic, Juan de Fuca, Indian, and East Pacific Rise ridges. The MORB data are plotted along with arc data in Fig. 10a in terms of V/Sc versus MgO. V/Sc ratios appear to increase slightly with degree of magmatic differentiation (decreasing MgO content) at MgO < 8 wt %. As shown in Fig. 7, the increase in V/Sc is probably due to the onset of clinopyroxene crystallization.

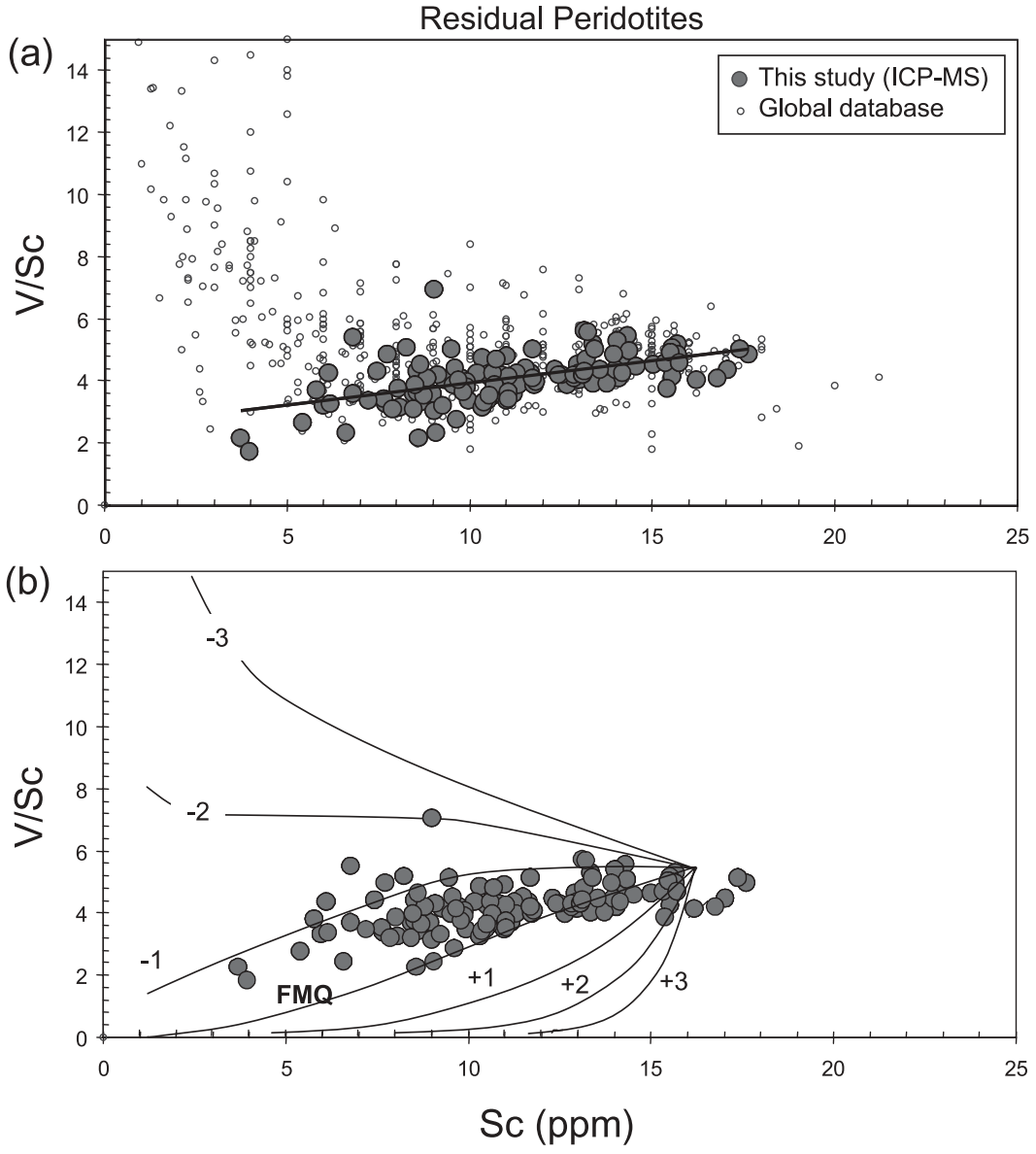

Fig. 9. (a) Whole-rock V/Sc versus Sc data for peridotites from this study (filled circles) compared with the global literature database (open circles). The continuous line represents a regression to the peridotite data from this study only. (b) V/Sc and Sc data (this study) plotted with fO_2 melting isopleths from Fig. 6b (reported as ΔFMQ values).

However, if we consider only those samples with MgO contents between 8 and 12 wt %, we capture those samples that have primarily experienced only olivine (and minor spinel) crystallization, which has little influence on melt V/Sc ratio because both elements are highly incompatible in olivine. Thus, V/Sc ratios of basalts with MgO contents between 8 and 12 wt % probably come close to representing that of their magmatic parent, and provide a window to mantle fO_2. The MgO-filtered V/Sc data are shown as a frequency distribution in Fig. 10b. The range in MgO-filtered V/Sc ratios decreases substantially, yielding an average V/Sc ratio of 6·7 ± 1·1 (1σ).

Superimposed on Fig. 10a and b are the calculated V/Sc ratios for given fO_2s at $F = 10$ wt %. If the assumptions in our melting model are reasonable, then the narrow range in V/Sc implies that the fO_2 of the MORB source is constrained roughly between FMQ–1 and FMQ+0·2. The model predictions fall within the range of fO_2 estimated from the Fe^{2+}/Fe^{3+} ratios of minerals and glasses in abyssal peridotites and MORB, respectively [FMQ–2·5 to FMQ+0·5; (Christie *et al.*, 1986; Wood *et al.*, 1990)]. The fO_2s predicted for MORB by the V/Sc redox method are also self-consistent with the redox conditions predicted by the same method for peridotites.

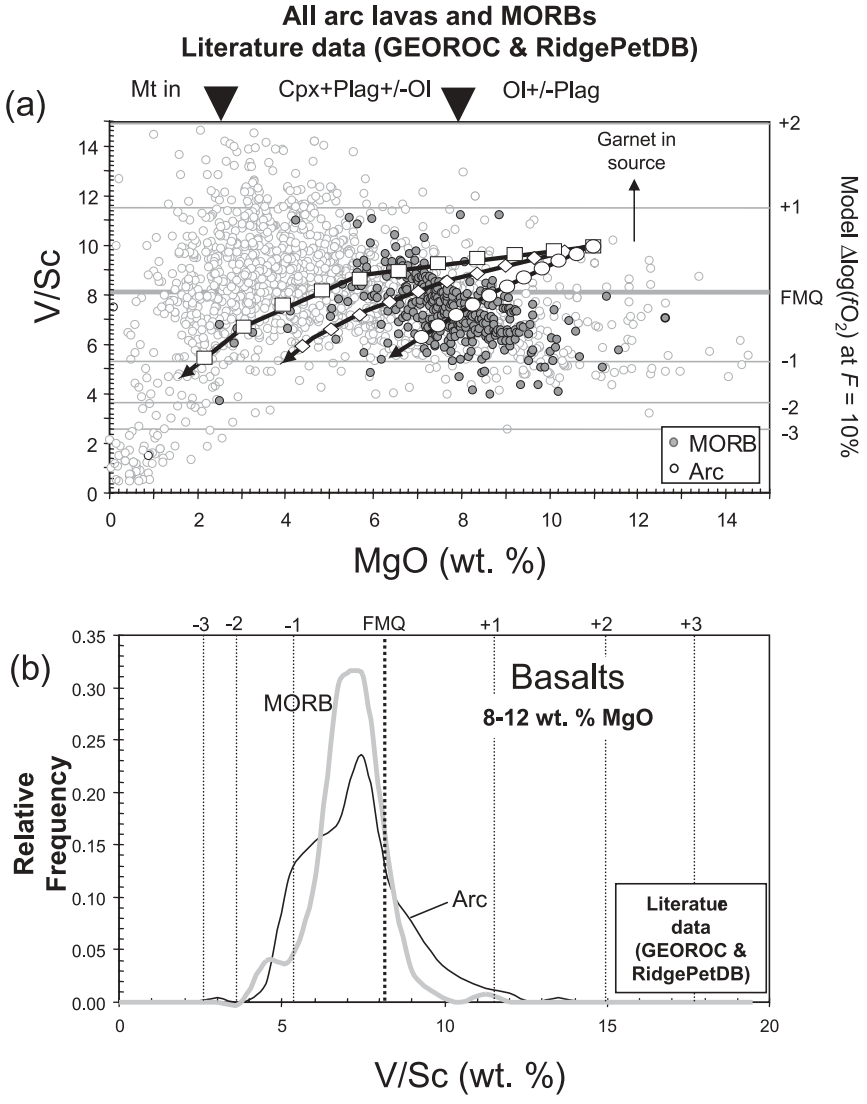

Fig. 10. (a) Whole-rock V/Sc versus MgO (wt %) in mid-ocean ridge basalts (MORB) and arc lavas from the global literature database (GEOROC and RidgePetDB). Horizontal lines represent model fO_2–V/Sc contours at melt fraction $F = 10$ wt % (right vertical axis). Top horizontal axis is divided into three parts corresponding to the appearance of different crystallizing phases (Ol, olivine; Plag, plagioclase; Cpx, clinopyroxene; Mt, magnetite). The three curved black lines represent (from left to right) mixing lines between a lava having a hypothetically high primary V/Sc with estimated upper, average and lower continental crust (Rudnick & Fountain, 1995); symbols are at 10% increments. Vertical arrow shows the direction in which V/Sc would increase if melting took place in the garnet stability field (see Fig. 8). (b) Normalized frequency histogram for V/Sc for MORB and arc lavas with MgO contents between 8 and 12 wt % MgO. Vertical lines represent the fO_2–V/Sc contours at $F = 10$ wt %, as in (a).

Arc lavas (literature data and this study)

Global literature database (GEOROC)

We now examine the V/Sc systematics of arc magmas, beginning with the GEOROC database. In the next section, we examine the Cascades magmatic series in more detail. Pre-compiled datasets for the following arcs were used: Aleutian, Andean, Cascades, Central American, Izu–Bonin, Kamchatka, Luzon, Marianas, Mexican and Tonga arcs. The Cascades, Central American and Mexican arcs correspond to regions where young, hot oceanic lithosphere is being subducted. In contrast, the western Pacific arcs (Izu–Bonin, Kamchatka, Luzon, Marianas and Tonga) correspond to regions where old, cold lithosphere is being subducted. The pre-compiled files were filtered to eliminate any non-magmatic rocks (e.g. sediments, xenoliths, cumulates) that were accidentally incorporated into the database. We also eliminated any samples (e.g. fore-arc, oceanic crust, seamounts, etc.) that do not specifically represent arc lavas.

Figure 10a contrasts all arc and MORB data in terms of V/Sc versus MgO. The arc lavas can be subdivided

into three parts. For MgO > 8 wt %, V/Sc ratios appear to be roughly constant over a range in MgO. Between 3 and 8 wt % MgO, the scatter in V/Sc ratios increases substantially and the average V/Sc ratio increases. Finally, below ~3% MgO, V/Sc plummets. These systematics can be rationalized as follows. At MgO > 8 wt %, the main crystallizing phase is olivine, which does not significantly change the V/Sc ratio of the melt, for reasons discussed above. At MgO between ~3 and 8 wt %, most of the rise in V/Sc is attributed largely to the appearance of clinopyroxene as a crystallizing phase. For MgO < 4 wt %, the rapid decrease in V/Sc reflects the appearance of Fe–Ti oxide as a significant crystallizing phase, which strongly prefers V over Sc. The MgO > 8 wt % window thus represents the best estimate of the V/Sc ratio of the parent arc basalt (7·09 ± 2·5, 1σ; Fig. 10b). The V/Sc ratios of these high-MgO basalts can be compared with the V/Sc–fO_2 melting contours, as we did for MORB. As discussed previously, we treat primary arc lavas as if they are 10% melts, like MORB. This is consistent with similar Ti contents (inverse proxy for degree of melting, F) in primitive MORB and most arc lavas (Fig. 5b). Although some high-Mg-number [Mg/(Mg + Fe)] basaltic andesites and boninites may represent much higher-degree melts (up to 30%), these are volumetrically minor in most arcs (see Fig. 5a and b).

Figure 10a shows that basalts with the highest V/Sc ratios tend to be from arcs. However, independent of model assumptions, an unequivocal feature of Fig. 10a and b is that for MgO > 8 wt %, most of the V/Sc ratios of arc lavas overlap extensively with MORB. These results are consistent with a recent investigation, which shows that Ti/V, previously used to distinguish the tectonic affinities of magmatic rocks (Shervais, 1982), may not be adequate for distinguishing arc basalts and MORB (Vasconcelos-F. *et al.*, 2001). Like the peridotite perspective, the remarkable similarity in V/Sc ratios between arc and mid-ocean ridge basalts is surprising in light of the wide range of barometric fO_2s seen in arc lavas. If the V/Sc ratios of the arc basalts are representative of their mantle source regions, this implies that the primary mantle fO_2 beneath arcs is not very different from that beneath mid-ocean ridges (e.g. identical to within ±0·5 log units). Even if we consider some of the arc basalts with higher V/Sc ratios, the estimated V/Sc-inferred fO_2s are nowhere near as high as the corresponding barometric fO_2s of the arc lavas.

The Cascades: a closer look

In this section, we specifically focus on the Cascades magmatic arc to see if there are any petrogenetically significant systematics 'hidden' within the scatter of the global literature database. We chose a suite of primitive basalts from the Cascades volcanic arc in southern Washington (Smith & Leeman, 2005), southern Oregon and northern California (Bacon *et al.*, 1997; Grove *et al.*, 2002). The data represent samples from Mount Shasta and the Lassen volcanic field (northern California), Crater Lake (Oregon) and our own data from southern Washington. We have independently confirmed a few of Bacon *et al.*'s and Grove *et al.*'s data by re-analyzing some of their samples (see the Appendix); hence, we believe that this subset of data is internally consistent with ours.

The Cascades primitive magmatic series includes low-potassium tholeiitic to alkalic basalts of intraplate affinity, as well as calcalkalic basalts (Leeman *et al.*, 2005). The former are characterized by lower K_2O and Ba/Yb values than the calcalkalic basalts. In Fig. 11a, Ba/Yb ratios and K_2O contents for primitive basaltic magmas from the Cascades (SiO_2 < 52 wt %, MgO > 6 wt %) are positively correlated. Importantly, there appears to be no correlation between Ba/Yb and K_2O with MgO (not shown) content or TiO_2 content (Fig. 11b). Variations in MgO content are in part due to fractional crystallization, whereas variations in TiO_2 content in the most primitive lavas are due to differences in the degree of melting. The lack of correlations with MgO and TiO_2 thus indicate that Ba/Yb and K_2O reflect source compositions. It is widely assumed that Ba is a fluid-mobile element, and that high Ba/Yb ratios indicate the influence of fluids (Yb is not fluid-mobile). The variations in Ba/Yb and K_2O are believed to reflect different slab contributions from the sources for arc lavas (Leeman *et al.*, 2005).

An important feature is that there is a distinct correlation between V/Sc and Ba/Yb ratio (and K_2O; Fig. 11a) in primitive basalts (Fig. 12a). V/Sc ratios range from ~5 in the tholeiitic end-member (low Ba/Yb) to up to ~10–11 in the more calcalkalic end-members (high Ba/Yb). When the data are taken as a whole, there is no correlation between V/Sc and MgO content (Fig. 12b). Because it is unlikely that the V/Sc ratio of the mantle wedge has been significantly modified by fluid metasomatism, the variations in V/Sc for a given MgO must derive from partial melting processes and not variations in the V/Sc of the source. The two melting parameters that can affect V/Sc in the melt are variations in fO_2 and degree of melting. There appears to be no correlation between V/Sc and TiO_2 (not shown, but this can be inferred from Fig. 11b) in the Cascades magmas, so the latter is not considered here to be a significant effect. This suggests fO_2 may be the remaining parameter. If we now use the F = 10 wt % V/Sc–fO_2 contours, we find that the observed range in V/Sc ratio corresponds to an apparent fO_2 of melting between ~FMQ–1·25 and FMQ+0·5. This range coincides closely with that of MORB mantle, as inferred from V/Sc systematics (Fig. 8). Thus, whereas the apparent correlation between V/Sc and Ba/Yb in the Cascades magmatic series suggests that fluids indeed

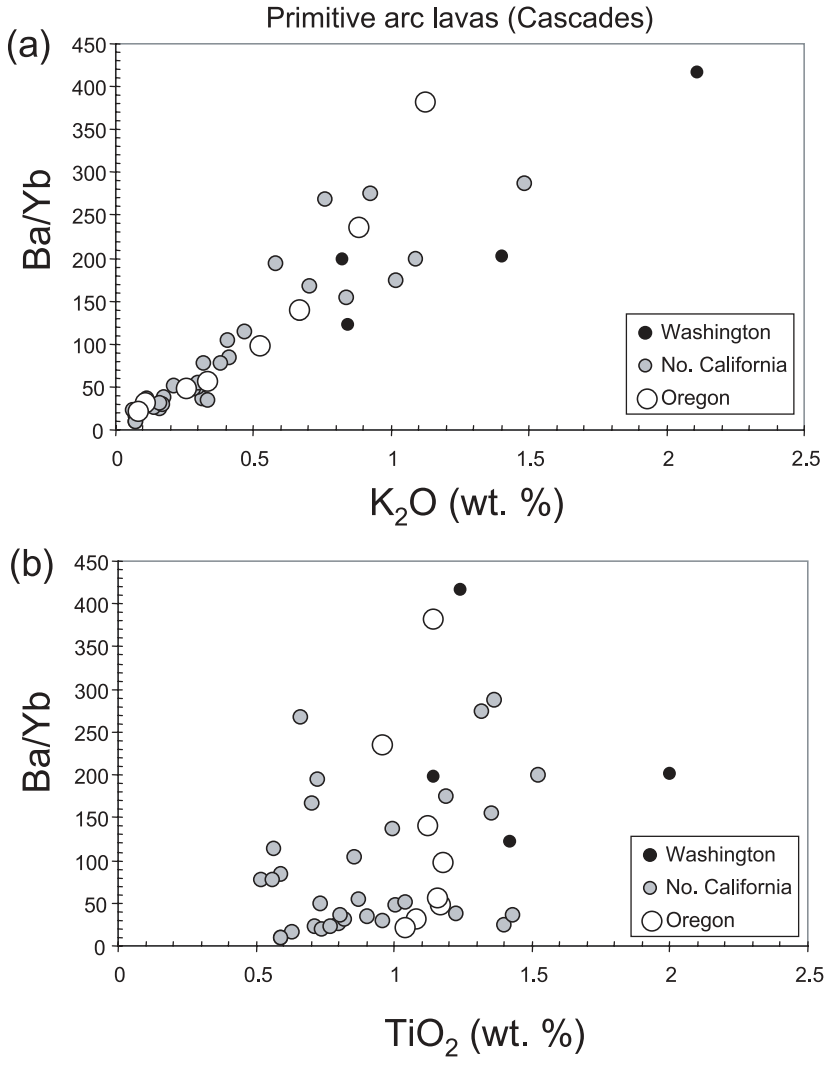

Fig. 11. (a) Ba/Yb versus K_2O (wt %) in primitive basalts from the Cascades magmatic arc series (7–12 wt % MgO). Lavas can be roughly subdivided on the basis of their K_2O contents (tholeiites have $K_2O < 0{\cdot}5\%$; most others are calcalkalic). Note that there is no correlation between Ba/Yb or K_2O with MgO content, indicating that Ba/Yb and K_2O reflect source signatures. (b) Ba/Yb versus TiO_2 (wt %) in primitive basalts from the Cascades.

influence fO_2 during melting, the overall effect is small. Importantly, the range in V/Sc ratios of primitive Cascade basalts spans most of the range seen in the global database of primitive arc basalts, reinforcing the suggestion in the previous section that arc lavas appear, on average, to derive from mantle of similar fO_2 to MORB mantle. However, of equal importance is the fact that upon closer inspection, subtle variations in arc source fO_2 may exist as a consequence of fluid metasomatism.

DISCUSSION

On the similarities in V/Sc ratios of arc lavas and MORB

The above case studies show that although there may be some correlation between primary mantle fO_2 and the amount of subduction-related fluids in arc environments, the overall range in primary mantle fO_2 inferred from V/Sc systematics is much smaller than the range in barometric fO_2 of the lavas. The most obvious question is whether this similarity may be an artifact of some process that tends to decrease the V/Sc ratio of arc lavas before or very early in the differentiation process. A number of factors come to mind. These are discussed in sequence below.

Crustal contamination in 'primitive' arc lavas

Continental crust is characterized by V/Sc ratios in the range of 4–6 (Rudnick & Fountain, 1995), hence its incorporation into a hypothetical arc basalt with a high V/Sc ratio (and hence originating from a mantle with high fO_2) would decrease the basalt's V/Sc ratio.

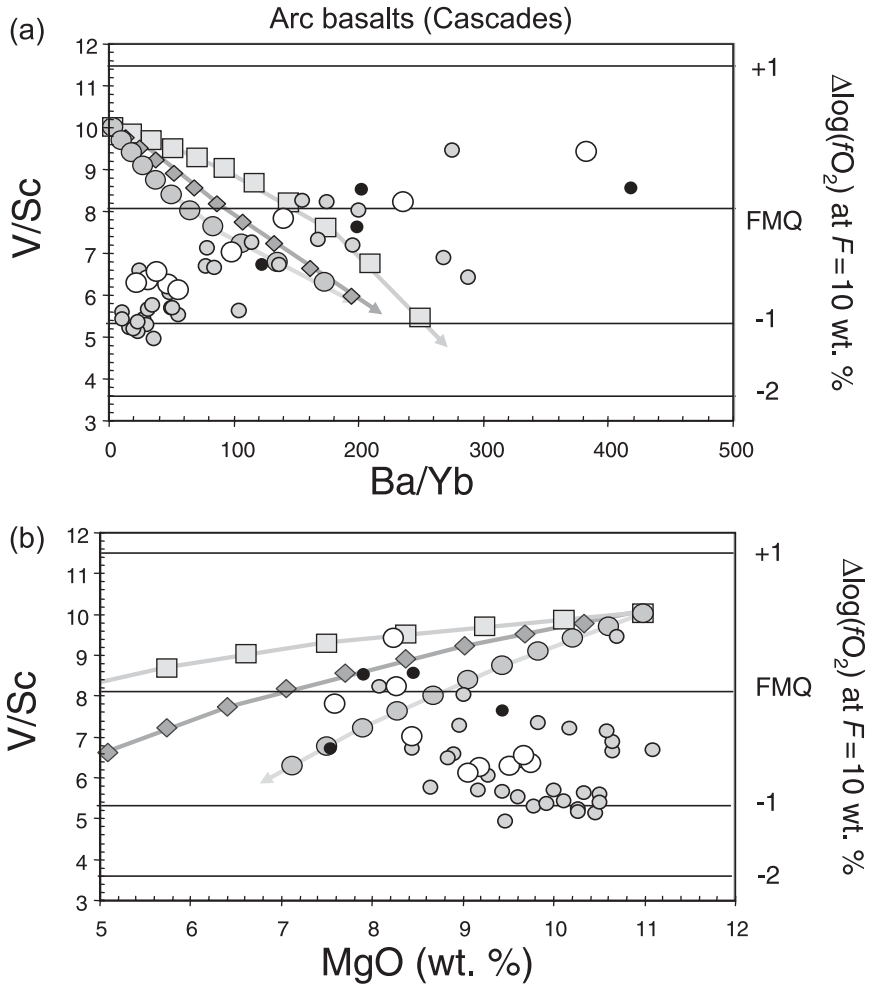

Fig. 12. (a) V/Sc in Cascade are basalts plotted against Ba/Yb. Horizontal continuous lines correspond to V/Sc–fO_2 melting contours at $F = 10$ wt %, as in Fig. 8. (b) V/Sc versus MgO (wt %) of Cascades magmatic arc series. Horizontal continuous lines correspond to V/Sc–fO_2 melting contours at $F = 10$ wt %, as in Fig. 8. Curves in (a) and (b) represent mixing lines between a hypothetical primary arc lava with high V/Sc and continental crust with symbols representing 10% increments (circles, lower continental crust; diamonds, bulk continental crust; squares, upper continental crust).

However, because the concentrations of V and Sc in continental crust are not significantly different from that in primitive basalts, unreasonable amounts (>50 wt %) of crustal contamination are needed to significantly decrease the V/Sc ratio of the basalt. Addition of such large amounts of crust would be manifested in distinct major element changes, such as a large decrease in MgO (Figs 10a and 12b) or an increase in SiO_2 content. Such mixing trajectories are not seen in arc lavas. Similarly, it can also be shown that the correlation between Ba/Yb and V/Sc seen in the Cascades magmas (Fig. 12a) cannot be explained by crustal contamination.

Garnet peridotite melting for arc lavas

The effect of melting in the garnet lherzolite stability field also cannot explain the low V/Sc ratios of arc lavas. As discussed earlier, melting of a garnet lherzolite yields a higher V/Sc ratio in the melt (Fig. 8).

Higher melting degrees for arc lavas

One of the assumptions in comparing the V/Sc ratios of primitive arc lavas and MORB is that their primary/parental magmas represent similar degrees of melting (e.g. 10%). At high degrees of melting, the fO_2 isopleths converge such that the sensitivity of the V/Sc ratio to fO_2 decreases. For example, if arc lavas actually represent 20% melts, their expected V/Sc ratios at fO_2s of FMQ+3 would be ~12, which itself would correspond to an fO_2 of only FMQ+1 if arc lavas were erroneously assumed to be 10% melts. Although this scenario may explain our observations, the problem is that arc lavas, in general, are probably not significantly higher-degree melts than

MORB. As shown in Fig. 5, the similar Cr and Ti systematics of primitive arc and MORB lavas suggest that, on average, arc lavas and MORB derive from similar degrees of melting.

High-pressure crystallization

Another possibility is that arc lavas begin differentiating at greater depths than MORB due to the thick pre-existing lithosphere through which they must pass. At high pressure, the olivine phase field contracts significantly so that other phases, such as clinopyroxene, will be more likely to crystallize. Clinopyroxene crystallization, however, would lead to an increase in V/Sc ratio, especially for fO_2s greater than FMQ.

It can be seen that all of the above complicating factors cannot explain the remarkable similarity in V/Sc ratios between primitive arc lavas and MORB. Crustal contamination is an ineffective means of decreasing the V/Sc ratio, whereas all of the other factors only serve to increase V/Sc. We thus conclude that the similarity in V/Sc ratios reflects a similarity in the primary fO_2s of the mantle source regions of MORB and primitive arc lavas.

Why do arc lavas and some arc xenoliths have higher barometric fO_2s than their primary fO_2s as inferred from V/Sc systematics?

Based on the above discussion, our preferred interpretation is that the V/Sc-inferred fO_2s of the mantle source regions to arc lavas are significantly lower than their corresponding barometric fO_2s. Similarly, some arc-related peridotite xenoliths appear to have higher barometric fO_2s than MORB-source mantle (though not as high as arc lavas), even though their V/Sc systematics imply MORB-like fO_2s. Below, we first discuss why arc lavas have barometric fO_2s that tend to be higher than the barometric fO_2s of arc xenoliths and the V/Sc-inferred fO_2s of the source regions to arc lavas. We leave the smaller discrepancy between V/Sc-inferred and barometric fO_2s of arc xenoliths to the end.

On the origin of high barometric fO_2 in arc lavas

The large discrepancy between the barometric fO_2s of arc lavas and the V/Sc-inferred fO_2s of their source regions suggests that the high fO_2s of arc lavas might be due to the evolution of magmatic fO_2 during ascent, emplacement and/or magmatic differentiation. Contamination by crustally derived fluids, dissociation of volatiles, fractional crystallization and hydrothermal alteration are all processes that could potentially modify fO_2 in the magma. Holloway (2004) recently hypothesized that rapidly crystallized magmas may undergo an auto-oxidation process in which ferrous iron is oxidized by water to generate magnetite and H_2, the latter of which is free to leave the system as a fluid:

$$3\mathrm{FeO(melt)} + \mathrm{H_2O(glass)} = \mathrm{FeO \times Fe_2O_3(magnetite)} + \mathrm{H_2(fluid)}. \quad (2)$$

This hypothesis was motivated by the observation that the crystallized parts of MORB tend to have higher ferric contents than the corresponding quenched rims (glass), even though the bulk compositions of the crystalline and glassy parts are nearly identical. The crystalline parts also appear to have internally crystallized magnetite. Loss of hydrogen by reaction (2) will result in an increase in ferric iron content. As a consequence, the ferric/ferrous ratio of a crystalline basalt is significantly higher than that in its magmatic state, and, as such, the inferred barometric fO_2 of the crystalline basalt will also be significantly higher than that in the magmatic state. Holloway pointed out that the amount of water in typical MORB glasses (0·1–0·4 wt %) is sufficient to explain the higher fO_2s of the crystallized portions of MORB compared with their glassy rims. Because the amount of water in arc lavas is generally higher than that of MORB, this auto-oxidation effect is even more likely to occur in arc lavas. For example, for an arc lava with 1·5–2·0 wt % H_2O, auto-oxidation could increase the fO_2 by two orders of magnitude (Holloway, 2004). If this auto-oxidation hypothesis is correct, it provides an attractive explanation for the higher fO_2s of arc lavas (which are invariably sampled in crystalline form) compared with their magma source regions. As auto-oxidation occurs in a closed system (except for loss of H_2), there would be no noticeable effects on bulk-rock chemistry (e.g. no changes in V and Sc contents).

This leaves us with the question of how much of the high barometric fO_2s seen in arc lavas is due to differentiation and degassing processes and how much is due to true fO_2 variations in their source regions. Our investigation of the Cascades arc magmas suggests that there may be fO_2 variations in the source regions by 1–1·5 orders of magnitude, but much larger source variations are not likely considering the global similarity in V/Sc systematics of arc lavas and MORB.

On the origin of high barometric fO_2 in mantle xenoliths

We now discuss why barometric fO_2s of mantle xenoliths tend to be more variable and reach higher values than those implied by their remarkably similar V–Sc systematics. As pointed out earlier, mantle xenoliths undoubtedly derive from the lithospheric mantle, as evidenced by the fact that nearly all mantle xenoliths have last equilibrated at subsolidus conditions. Because the lithospheric mantle is less mobile than the asthenospheric mantle, it remains isolated from the convecting mantle for much longer periods of time. For these reasons, the

trace-element composition of the lithospheric mantle often represents the time-integrated product of numerous metasomatic events. Given that most metasomatizing fluids are oxidizing (McGuire *et al.*, 1991; McCammon *et al.*, 2001), it seems reasonable to suggest that the fO_2 of lithospheric mantle could eventually be increased by the passage of numerous oxidizing, metasomatizing fluids. Because arc lithospheric mantle has a much longer residence time above a dehydrating slab than any given parcel of asthenospheric mantle wedge material, it is likely that arc lithosphere has interacted more with oxidizing fluids than the asthenospheric mantle itself. It is thus possible that arc lithosphere could become slightly more oxidized than the asthenospheric mantle. We suggest that the slightly high barometric fO_2s of some arc xenoliths may occur due to metasomatic resetting during long-term residence in the lithospheric mantle, whereas their low V/Sc-inferred fO_2s may reflect the original fO_2s attending partial melting of these xenoliths when they were part of the asthenosphere and not yet incorporated into the lithosphere.

If continental lithospheric mantle has been subsequently oxidized, it follows that melts of lithospheric mantle should yield higher V/Sc ratios, all other parameters being constant (e.g. initial V and Sc concentrations and average degree of melting). In this context, the positive correlation between V/Sc and Ba/Yb in primitive Cascades arc lavas could occur due to melting fluid-metasomatized asthenospheric mantle or melting fluid-metasomatized lithospheric mantle. Indeed, Leeman *et al.* (2005) have suggested that some arc basalts may acquire their compositions from melting or interaction with lithospheric mantle.

Is the asthenosphere buffered in fO_2?

Assuming that the fO_2 of dehydrating slab fluids is high (due to oxidation at the Earth's surface) and that fluids are probably more abundant in arc environments than beneath mid-ocean ridges, the low fO_2s of asthenospheric arc mantle, as inferred from V/Sc systematics, suggest that the fO_2 of the upper mantle may be globally buffered (e.g. the volume of oxidizing fluids is insufficient to overprint the asthenospheric mantle fO_2) and the oxidizing potential of slab fluids is not as high as widely perceived. It has been pointed out before that the oxidizing potential of water in the mantle is in fact very low, so other oxidizing agents are required (Frost & Ballhaus, 1998). Fe-bearing hydrous melts have been proposed by Mungall (2002) as more effective oxidizing agents, but it is unclear how pervasive such fluids are in subduction zone environments. According to Mungall, these fluids are likely to be released only when temperatures high enough to melt oceanic crust are achieved; such conditions are met only in the rare cases in which hot and young oceanic lithosphere is being subducted. Thus, if Mungall's hypothesis is correct, it means that, generally, the amount and oxidizing power of subduction-related fluids released into the sub-arc mantle wedge may be insufficient to exceed the buffering capacity of the asthenospheric mantle.

These observations suggest that the upper convecting mantle may be strongly buffered, supporting previous proposals of this concept (Blundy *et al.*, 1991). A buffered mantle is also in line with observations that the fO_2 of the mantle has also not changed significantly with time, as evidenced from V systematics of Archean komatiites, basalts and peridotites (Canil, 2002; Lee *et al.*, 2003; Li & Lee, 2004) and Cr systematics in Archean basalts and komatiites (Delano, 2001). Although it is beyond the scope of this paper to discuss in detail the different types of possible buffering assemblages, we note that assemblages involving H, C and S fluid species or Fe species equilibria have all been proposed. Which particular system controls fO_2 is, so far, equivocal given the uncertain abundances of some of these elements, and, thus, buffering capacity, in the mantle (Canil *et al.*, 1994). On a final note, we point out that continental lithospheric mantle, by contrast, may not be so well buffered, owing to the likelihood that the total flux of oxidizing metasomatic fluids through continental lithospheric mantle is much larger than that in the convecting mantle itself.

Caveats, concerns and continuing work

Several issues have not been addressed in great detail in this study. The first issue is that we considered a homogeneous source. Although we believe that, in general, this is a reasonable assumption, there are undoubtedly pockets of major-element heterogeneities in the mantle. For example, some xenolith suites contain ample evidence for metasomatic veins and dikes. Unlike cryptic metasomatism, which involves only changes in trace-element composition, veins and dikes reflect modal metasomatism. Not only might these veins or dikes be locally oxidizing, but they are also likely to have V and Sc contents differing from the primitive mantle and to have melting stoichiometries differing substantially from typical lherzolite. Some of these veins or dikes are rich in hydrous minerals, such as amphibole or phlogopite. The V/Sc ratios of such magmas will be difficult to interpret because of the added free parameters in the modelling (e.g. initial V and Sc content, melting stoichiometry and partitioning of V and Sc in hydrous phases are at present ill-constrained). Given all these free parameters and the remarkable similarity in V/Sc systematics of most arc basalts and MORB, it seems highly unlikely that melting of unusual metasomatic veins plays a significant role in the generation of MORB and arc lavas. However, unusually hydrous lavas in arc and intraplate settings might indeed originate from melting of such veins. We note that intraplate lavas appear to have much greater variation in V/Sc ratios, including values

much greater (>9) than those seen in MORB and most arc basalts. These higher values could imply higher fO_2s during melting, lower degrees of melting, the presence of residual garnet, and/or different V and Sc contents of the source. For such magmas, V and Sc systematics should be carefully examined in conjunction with other trace and major elements in order to unravel these complexities. If these complexities can be dealt with, V/Sc studies of intraplate lavas derived from lithospheric melting may help to constrain the fO_2 of the lithospheric mantle, which would be especially helpful in those regions in which mantle xenoliths are absent.

Finally, a methodical study of V/Sc systematics in conjunction with barometric determinations of fO_2 in a continuous magmatic differentiation series would go far in unraveling the evolution of fO_2 during magmatic differentiation. This approach would entail not only measuring bulk-rock V/Sc ratios, but also estimating empirically the partition coefficients of phenocryst–lava pairs at different stages of the magma differentiation history. These studies could also be combined with other redox-sensitive elements, e.g. Cr and Eu.

CONCLUSIONS

An in-depth examination of V/Sc systematics in primitive arc lavas shows that V/Sc is correlated with fluid-mobile element enrichment (K, Ba), indicating that mantle fO_2 may be subtly influenced by the addition of fluids to the mantle wedge. Nevertheless, it appears that, on average, MORB and many arc magmas have indistinguishable V/Sc systematics within error, resulting in similar fO_2s (FMQ–1·25 to FMQ+0·5) predicted for their source regions. The V/Sc systematics of peridotites from different localities and tectonic environments, with varying degrees of metasomatic alteration, also show remarkably similar V/Sc systematics. The peridotite V/Sc data correspond to predicted fO_2s ranging from FMQ–1·25 to FMQ, completely overlapping with the range seen in MORB and arc lavas. Thus, despite a small influence of fluids on fO_2 in subduction zones, the fO_2 of the asthenospheric mantle is, on average, surprisingly homogeneous. In the case of MORB, the V/Sc fO_2s coincide with barometric fO_2s for abyssal peridotites and MORB glasses. In the case of arc magmas, the V/Sc fO_2s are lower than the high barometric fO_2s seen in arc lavas and some arc-related mantle xenoliths. These observations suggest that the upper mantle is largely buffered in terms of fO_2. High barometric fO_2s in mantle xenoliths and arc lavas can be explained if the former receive a much larger time-integrated fluid flux due to their long residence times in the lithospheric mantle, and if the latter have become oxidized during magma ascent and differentiation. A buffered mantle implies that secular changes in mantle fO_2 are likely to be small.

ACKNOWLEDGEMENTS

Support from NSF grants (EAR 0309121, 0440033, 0003612 and 0409423) to Lee and Leeman and NSERC of Canada and Yukon Geology Program grants to Canil are acknowledged. M. Hu is thanked for help with data compilation. Kevin Righter and an anonymous reviewer are thanked for thoughtful comments. Discussions with Chip Lesher, Lara Heister, Terry Plank, Mark Little, Yongsheng Liu and Alan Brandon are greatly appreciated. Alan Brandon and Marc Norman are also thanked for contributing the data analyzed at Australia National University. We also thank Tim Grove for providing splits of lavas from the Northern California Cascades used to confirm inter-laboratory agreement.

REFERENCES

Bacon, C. R., Bruggman, P. E., Christiansen, R. I., Clynne, M. A., Donnelly-Nolan, J. M. & Hildreth, W. (1997). Primitive magmas at five Cascade volcanic fields: melts from hot, heterogeneous sub-arc mantle. *Canadian Mineralogist* **35**, 397–423.

Baker, M. B., Grove, M. & Price, R. (1994). Primitive basalts and andesites from the Mt. Shasta region, N. California: products of varying melt fraction and water content. *Contributions to Mineralogy and Petrology* **118**, 111–129.

Ballhaus, C., Berry, R. F. & Green, D. H. (1990). Oxygen fugacity controls in the Earth's upper mantle. *Nature* **348**, 437–440.

Ballhaus, C., Berry, R. F. & Green, D. H. (1991). High pressure experimental calibration of the olivine–orthopyroxene–spinel oxygen geobarometer: implications for the oxidation state of the upper mantle. *Contributions to Mineralogy and Petrology* **107**, 27–40.

Beattie, P., Ford, C. & Russell, D. (1991). Partition coefficients for olivine–melt and orthopyroxene–melt systems. *Contributions to Mineralogy and Petrology* **109**, 212–224.

Blatter, D. L. & Carmichael, I. S. E. (1998). Hornblende peridotite xenoliths from central Mexico reveal the highly oxidized nature of subarc upper mantle. *Geology* **26**, 1035–1038.

Blundy, J. D., Brodholt, J. P. & Wood, B. J. (1991). Carbon–fluid equilibria and the oxidation state of the upper mantle. *Nature* **349**, 321–324.

Brandon, A. D. & Draper, D. S. (1996). Constraints on the origin of the oxidation state of mantle overlying subduction zones: an example from Simcoe, Washington, USA. *Geochimica et Cosmochimica Acta* **60**, 1739–1749.

Canil, D. (2002). Vanadium in peridotites, mantle redox and tectonic environments: Archean to present. *Earth and Planetary Science Letters* **195**, 75–90.

Canil, D. (2004). Mildly incompatible elements in peridotites and the origins of mantle lithosphere. *Lithos* **77**, 375–393.

Canil, D. & Fedortchouk, Y. (2000). Clinopyroxene–liquid partitioning for vanadium and the oxygen fugacity during formation of cratonic and oceanic mantle lithosphere. *Journal of Geophysical Research* **105**, 26003–26016.

Canil, D., O'Neill, H. S. C., Pearson, D. G., Rudnick, R. L., McDonough, W. F. & Carswell, D. A. (1994). Ferric iron in peridotites and mantle oxidation states. *Earth and Planetary Science Letters* **123**, 205–220.

Carmichael, I. S. E. (1991). The redox states of basic and silicic magmas: a reflection of their source regions? *Contributions to Mineralogy and Petrology* **106**, 129–141.

Christie, D. M., Carmichael, I. S. E. & Langmuir, C. H. (1986). Oxidation states of mid-ocean ridge basalt glasses. *Earth and Planetary Science Letters* **79**, 397–411.

Delano, J. W. (2001). Redox history of the Earth's interior since ~3900 Ma: implications for prebiotic molecules. *Origins of Life and Evolution of the Biosphere* **31**, 311–341.

Eggins, S. M., Woodhead, J. D., Kinsley, L., Mortimer, G. E., Sylvester, P., McCulloch, M. T., Hergt, J. M. & Handler, M. R. (1997). A simple method for the precise determination of >40 trace elements in geological samples by ICP-MS using enriched isotope internal standardisation. *Chemical Geology* **134**, 311–326.

Frost, B. R. (1991). Introduction to oxygen fugacity and its petrologic importance. In: Lindsley, D. H. (ed.) *Oxide Minerals: Petrologic and Magnetic Significance. Mineralogical Society of America, Reviews in Mineralogy* **25**, 1–9.

Frost, B. R. & Ballhaus, C. (1998). Comment on 'Constraints on the origin of the oxidation state of mantle overlying subduction zones: an example from Simcoe, Washington, USA' by A. D. Brandon and D. S. Draper. *Geochimica et Cosmochimica Acta* **62**, 329–331.

Ghiorso, M. S., Hirschmann, M. M., Reiners, P. W. & Kress, V. C. (2002). The pMELTS: a revision of MELTS for improved calculation of phase relations and major element partitioning related to partial melting of the mantle to 3 GPa. *Geochemistry, Geophysics, Geosystems* **3**, 10.1029/2001GC000217.

Griffin, W. L., O'Reilly, S. Y. & Ryan, C. G. (1999). The composition and origin of sub-continental lithospheric mantle. In: *Mantle Petrology: Field Observations and High Pressure Experimentation: a Tribute to R. (Joe) Boyd. Geochemical Society, Special Publication* **6**, 13–45.

Grove, T. L., Parman, S. W., Bowring, S. A., Price, R. C. & Baker, M. B. (2002). The role of an H_2O-rich fluid component in the generation of primitive basaltic andesites and andesites from the Mt. Shasta region, N California. *Contributions to Mineralogy and Petrology* **142**, 375–396.

Hart, S. R. & Dunn, T. (1993). Experimental cpx/melt partitioning of 24 trace elements. *Contributions to Mineralogy and Petrology* **113**, 1–8.

Hauri, E. H., Wagner, T. P. & Grove, T. L. (1994). Experimental and natural partitioning of Th, U, Pb and other trace elements between garnet, clinopyroxene and basaltic melts. *Chemical Geology* **117**, 149–166.

Hofmann, A. W. (1988). Chemical differentiation of the Earth: the relationship between mantle, continental crust, and oceanic crust. *Earth and Planetary Science Letters* **90**, 297–314.

Holloway, J. R. (2004). Redox reactions in seafloor basalts: possible insights into silicic hydrothermal systems. *Chemical Geology* **210**, 225–230.

Jones, J. H. (1995). Experimental trace element partitioning. In: Ahrens, T. J. (ed.) *Rock Physics and Phase Relations, American Geophysical Union, Geodynamic Series* **3**, 73–104.

Jordan, T. H. (1975). The continental tectosphere. *Geophysics and Space Physics* **13**, 1–12.

Kress, V. C. & Carmichael, I. S. E. (1991). The compressibility of silicate liquids containing Fe_2O_3 and the effect of composition, temperature, oxygen fugacity and pressure on their redox states. *Contributions to Mineralogy and Petrology* **108**, 82–92.

Langmuir, C., Klein, E. M. & Plank, T. (1992). *Petrological Systematics of Mid-ocean Ridge Basalts: Constraints on Melt Generation Beneath Ocean Ridges. Geophysical Monograph, American Geophysical Union* **71**, 183–280.

Lee, C.-T., Yin, Q.-Z., Rudnick, R. L., Chesley, J. T. & Jacobsen, S. B. (2000). Os isotopic evidence for Mesozoic removal of lithospheric mantle beneath the Sierra Nevada, California. *Science* **289**, 1912–1916.

Lee, C.-T., Yin, Q., Rudnick, R. L. & Jacobsen, S. B. (2001*a*). Preservation of ancient and fertile lithospheric mantle beneath the southwestern United States. *Nature* **411**, 69–73.

Lee, C.-T., Rudnick, R. L. & Brimhall, G. H. (2001*b*). Deep lithospheric dynamics beneath the Sierra Nevada during the Mesozoic and Cenozoic as inferred from xenolith petrology. *Geochemistry, Geophysics, Geosystems* **2**, 2001GC000152.

Lee, C.-T. A., Brandon, A. D. & Norman, M. D. (2003). Vanadium in peridotites as a proxy for paleo-fO_2 during partial melting: prospects, limitations, and implications. *Geochimica et Cosmochimica Acta* **67**, 3045–3064.

Leeman, W. P., Lewis, J. F., Evarts, R. C., Conrey, R. M. & Streck, M. J. (2005). Petrologic constraints on the thermal structure of the southern Washington Cascades. *Journal of Volcanological and Geothermal Research* **140**, 67–105.

Lehnert, K., Su, Y., Langmuir, C. H., Sarbas, B. & Nohl, U. (2000). A global geochemical database structure for rocks. *Geochemistry, Geophysics, Geosystems* **1**, 1999GC000026.

Li, Z.-X. A. & Lee, C.-T. A. (2004). The constancy of upper mantle fO_2 through time inferred from V/Sc ratios in basalts. *Earth and Planetary Science Letters* **228**, 483–493.

Mathez, E. A. (1984). Influence of degassing on oxidation states of basaltic magmas. *Nature* **310**, 371–375.

Mattioli, G. S. & Wood, B. J. (1986). Upper mantle oxygen fugacity recorded by spinel lherzolites. *Nature* **322**, 626–628.

McCammon, C. A., Griffin, W. L., Hee, S. H. & O'Neill, H. S. C. (2001). Oxidation during metasomatism in ultramafic xenoliths from the Wesselton kimberlite, South Africa: implications for the survival of diamond. *Contributions to Mineralogy and Petrology* **141**, 287–296.

McDonough, W. F. & Sun, S.-S. (1995). The composition of the Earth. *Chemical Geology* **120**, 223–253.

McGuire, A. V., Dyar, M. D. & Nielson, J. E. (1991). Metasomatic oxidation of upper mantle peridotite. *Contributions to Mineralogy and Petrology* **109**, 252–264.

Mukasa, S. B. & Wilshire, H. G. (1997). Isotopic and trace element compositions of upper mantle and lower crustal xenoliths, Cima volcanic field, California: implications for evolution of the subcontinental lithospheric mantle. *Journal of Geophysical Research* **102**, 20133–20148.

Mungall, J. E. (2002). Roasting the mantle: slab melting and the genesis of major Au and Au-rich Cu deposits. *Geology* **30**, 915–918.

O'Reilly, S. Y., Griffin, W. L., Djomani, Y. H. & Morgan, P. (2001). Are lithospheres forever? Tracking changes in subcontinental lithospheric mantle through time. *GSA Today* **11**, 4–10.

Parkinson, I. J. & Arculus, R. J. (1999). The redox state of subduction zones: insights from arc-peridotites. *Chemical Geology* **160**, 409–423.

Pearson, D. G., Carlson, R. W., Shirey, S. B., Boyd, F. R. & Nixon, P. H. (1995). Stabilisation of Archaean lithospheric mantle: a Re–Os isotope study of peridotite xenoliths from the Kaapvaal craton. *Earth and Planetary Science Letters* **134**, 341–357.

Rudnick, R. L. & Fountain, D. M. (1995). Nature and composition of the continental crust: a lower crustal perspective. *Reviews of Geophysics* **33**, 267–309.

Sato, M. & Wright, T. L. (1996). Oxygen fugacities directly measured in magmatic gases. *Science* **153**, 1103–1105.

Shervais, J. W. (1982). Ti–V plots and petrogenesis of modern and ophiolitic lavas. *Earth and Planetary Science Letters* **59**, 101–118.

Smith, D. R. & Leeman, W. P. (2005). Chromian spinel–olivine phase chemistry and the origin of primitive basalts of the southern Washington Cascades. *Journal of Volcanological and Geothermal Research* **140**, 49–66.

Sugawara, T. (2000). Empirical relationships between temperature, pressure, and MgO content in olivine and pyroxene saturated liquid. *Journal of Geophysical Research* **105**, 8457–8472.

Sun, S. S. & McDonough, W. F. (1989). Chemical and isotopic systematics of oceanic basalts: implications for mantle composition and

processes. In: Saunders, A. D. & Norry, M. J. (eds), *Magmatism in the Ocean Basins*. *Geological Society*, *London*, *Special Publications* **42**, 313–345.

Vasconcelos-F., M., Verma, S. P. & Carmen Vargas-B., Y. R. (2001). Diagrama Ti–V: una nueva propeusta de discriminacion para magmas basicos en cinco ambientes tectonicos. *Revista Mexicana de Ciencias Geologicas* **18**, 162–174.

Walter, M. J. (1998). Melting of garnet peridotite and the origin of komatiite and depleted lithosphere. *Journal of Petrology* **39**, 29–60.

Wilshire, H. G., Meyer, C. E., Nakata, J. K., Calk, L. C., Shervais, J. W., Nielson, J. E. & Schwarzman, E. C. (1988). Mafic and ultramafic xenoliths from volcanic rocks of the western United States. *US Geological Survey*, *Professional Papers* **1443**, 179.

Wood, B. J. & Virgo, D. (1989). Upper mantle oxidation state: ferric iron contents of lherzolite spinels by ^{57}Mössbauer spectroscopy and resultant oxygen fugacities. *Geochimica et Cosmochimica Acta* **53**, 1277–1291.

Wood, B. J., Bryndzia, L. T. & Johnson, K. E. (1990). Mantle oxidation state and its relationship to tectonic environment and fluid speciation. *Science* **248**, 337–345.

APPENDIX

The new ICP-MS measurements are given in Tables A1 and A2. Table A1 consists of xenolithic and ophiolitic peridotites from scattered localities extending from the southwestern United States to the Canadian Cordillera and Alaska. Some of the xenolith localities have been previously described in the literature (Wilshire *et al.*, 1988; Mukasa & Wilshire, 1997). Nearly all samples are spinel peridotites, but a few contain both spinel and garnet (Big Creek, California; Lee *et al.*, 2000; Lee *et al.*, 2001*b*). Some ophiolitic samples (e.g. Feather River Ophiolite, California) have been variably serpentinized. These samples are included to show that V and Sc systematics are not significantly disturbed during serpentinization. The data in Table A1 were analyzed in three different ICP-MS laboratories and are referenced in Table A1 as (1) Rice University; (2) University of Victoria; (3) Australia National University. All measurements were determined by external standard normalization to an international rock standard. The data from Australia National University were previously published by Lee *et al.* (2003). However, during the course of this study, we discovered that the preferred V value for the external standard (United States Geological Survey Hawaiian Basalt standard BHVO-1) used in those measurements was lower (281 ppm) than that used in the laboratories at Rice University and University of Victoria (321 ppm; Eggins *et al.*, 1997). We have thus made a small correction to these numbers. The normalization value of BHVO-1 for Sc was taken to be 31·8 (Eggins *et al.*, 1997).

Table A2 consists of data for basaltic lavas from Mount Shasta in northern California and the southern Washington Cascades. We re-analyzed some of the samples from Bacon *et al.* (1997) and Grove *et al.* (2002). Their data are shown for comparison. In general, the agreement is very good.

Table A1: Peridotite V and Sc data

Sample name	Sample locality	Class	Rock type	Sc	V	V/Sc	Analyst*
California							
BC77	Big Creek, Sierra Nevada	x	sp–gt	8·98	62·5	6·96	1
1026V	Big Creek, Sierra Nevada	x	sp–gt	17·62	86·6	4·91	1
P7	Big Creek, Sierra Nevada	x	sp–gt	12·94	59·2	4·58	1
P10	Big Creek, Sierra Nevada	x	sp–gt	6·75	36·6	5·42	1
BC98-2	Big Creek, Sierra Nevada	x	sp	10·67	43·0	4·03	1
OK98-3	Oak Creek, Sierra Nevada	x	sp	13·35	69·6	5·22	1
OK98-9	Oak Creek, Sierra Nevada	x	sp	14·32	78·7	5·50	1
OK98-4	Oak Creek, Sierra Nevada	x	sp	15·65	81·3	5·20	1
Ki5-1	Cima Volcanic Field	x	sp	10·97	37·5	3·42	1
Ki5-8	Cima Volcanic Field	x	sp	15·55	79·5	5·11	1
Ki5-16	Cima Volcanic Field	x	sp	5·95	19·1	3·21	1
Ki5-31	Cima Volcanic Field	x	sp	11·28	46·8	4·15	1
Ki5-32	Cima Volcanic Field	x	sp	12·63	49·5	3·92	1
Ki5-45	Cima Volcanic Field	x	sp	8·54	37·1	4·34	1
Ki5-110	Cima Volcanic Field	x	sp	5·78	21·7	3·76	1
CiP98-8	Cima Volcanic Field	x	sp	12·31	54·0	4·39	1
CiP98-19	Cima Volcanic Field	x	sp	7·43	32·1	4·32	1
CiP98-62	Cima Volcanic Field	x	sp	10·84	46·0	4·24	1
CiP98-66	Cima Volcanic Field	x	sp	15·00	68·6	4·57	1
Ba-4–42	Dish Hill Cinder Cone	x	sp	17·36	88·0	5·07	3

Sample name	Sample locality	Class	Rock type	Sc	V	V/Sc	Analyst*
Ba-5–8	Dish Hill Cinder Cone	x	sp	12·98	52·6	4·05	3
Ba-5–17	Dish Hill Cinder Cone	x	sp	15·54	64·9	4·17	3
Ba-5–18	Dish Hill Cinder Cone	x	sp	13·91	58·6	4·21	3
DH 1	Dish Hill Cinder Cone	x	sp	8·41	30·5	3·63	3
DH-3	Dish Hill Cinder Cone	x	sp	16·20	65·7	4·06	3
DH 5	Dish Hill Cinder Cone	x	sp	12·85	53·3	4·15	3
DH 6	Dish Hill Cinder Cone	x	sp	10·57	36·9	3·49	3
DH-10	Dish Hill Cinder Cone	x	sp	14·29	67·0	4·68	3
DH 11	Dish Hill Cinder Cone	x	sp	12·50	53·0	4·24	3
DH 14	Dish Hill Cinder Cone	x	sp	12·41	52·4	4·22	3
CT1-1	Feather River Ophiolite	o	serp	10·53	44·2	4·20	1
CT1-2	Feather River Ophiolite	o	serp	12·98	55·6	4·29	1
CT3	Feather River Ophiolite	o	serp	12·82	54·3	4·23	1
CT7	Feather River Ophiolite	o	serp	10·98	53·0	4·83	1
CT10	Feather River Ophiolite	o	serp	6·76	24·5	3·62	1
Ct11	Feather River Ophiolite	o	serp	8·93	32·4	3·63	1
CT19	Feather River Ophiolite	o	serp	10·33	49·7	4·81	1
CT23	Feather River Ophiolite	o	serp	14·07	57·9	4·12	1
CT29	Feather River Ophiolite	o	serp	6·09	26·2	4·30	1
CT34	Feather River Ophiolite	o	serp	11·60	49·1	4·23	1
NB2a	Feather River Ophiolite	o	serp	9·73	40·2	4·13	1
NB8	Feather River Ophiolite	o	serp	11·65	50·1	4·30	1
NB8	Feather River Ophiolite	o	serp	11·65	50·1	4·30	1
NB10	Feather River Ophiolite	o	serp	9·28	37·8	4·08	1
NB10B	Feather River Ophiolite	o	serp	13·37	53·2	3·98	1
NB15	Feather River Ophiolite	o	serp	8·22	41·9	5·10	1
NB22	Feather River Ophiolite	o	serp	11·49	51·1	4·45	1
NB24	Feather River Ophiolite	o	serp	9·11	38·4	4·22	1
NB25	Feather River Ophiolite	o	serp	11·26	48·2	4·28	1
NB28	Feather River Ophiolite	o	serp	9·47	47·9	5·06	1
Nevada							
LC 1	Lunar Crater	x	sp	7·67	25·5	3·32	3
LC 25	Lunar Crater	x	sp	11·17	40·3	3·61	3
LC 47	Lunar Crater	x	sp	14·28	65·3	4·57	3
LC 52	Lunar Crater	x	sp	8·06	25·6	3·18	3
LC 62	Lunar Crater	x	sp	9·53	37·3	3·92	3
LC 69	Lunar Crater	x	sp	9·58	42·4	4·42	3
Arizona							
VT 6	Vulcan's Throne	x	sp	6·13	20·2	3·29	3
VT 18	Vulcan's Throne	x	sp	11·31	44·3	3·92	3
VT 19	Vulcan's Throne	x	sp	8·62	28·7	3·33	3
VT 26	Vulcan's Throne	x	sp	5·42	14·5	2·67	3
VT 29	Vulcan's Throne	x	sp	8·51	31·2	3·66	3
VT 30	Vulcan's Throne	x	sp	6·57	15·5	2·36	3
VT 44	Vulcan's Throne	x	sp	13·72	54·1	3·94	3
VT 45	Vulcan's Throne	x	sp	7·61	26·4	3·48	3
New Mexico							
KIL 1	Kilbourne Hole	x	sp	13·15	61·8	4·70	3
KIL 2	Kilbourne Hole	x	sp	13·97	61·5	4·40	3

Table A1: continued

Sample name	Sample locality	Class	Rock type	Sc	V	V/Sc	Analyst*
KIL 41	Kilbourne Hole	x	sp	10·16	43·4	4·27	3
KIL 70	Kilbourne Hole	x	sp	15·35	70·6	4·60	3
KIL 7	Kilbourne Hole	x	sp	13·54	59·8	4·42	3
Washington							
SIM 2	Simcoe	x	sp	8·43	26·4	3·13	3
SIM-5	Simcoe	x	sp	9·88	39·4	3·99	3
SIM 11	Simcoe	x	sp	8·98	27·6	3·07	3
SIM 12	Simcoe	x	sp	9·25	29·8	3·23	3
SIM 17	Simcoe	x	sp	11·02	45·9	4·17	3
SIM 20	Simcoe	x	sp	3·70	8·2	2·22	3
SIM 24	Simcoe	x	sp	9·61	26·8	2·78	3
SIM 25	Simcoe	x	sp	8·57	19·0	2·22	3
SIM 26	Simcoe	x	sp	7·71	37·9	4·91	3
SIM 28	Simcoe	x	sp	8·72	31·2	3·58	3
Northern Cordillera							
DC0212	Harz Pk (Yukon)	o	sp	10·62	45·6	4·29	2
DC0214	Harz Pk (Yukon)	o	sp	13·05	55·3	4·24	2
DC0216	Harz Pk (Yukon)	o	sp	11·76	46·1	3·92	2
DC0225	Harz Pk (Yukon)	o	sp	13·42	68·0	5·06	2
DC0228	Harz Pk (Yukon)	o	sp	10·64	41·7	3·92	2
DC0310	Perido Pk (Brit. Col.)	o	sp	17·03	75·0	4·40	2
DC0312	Perido Pk (Brit. Col.)	o	sp	15·69	77·1	4·91	2
DC0313	Perido Pk (Brit. Col.)	o	sp	15·49	76·4	4·93	2
DC0313d	Perido Pk (Brit. Col.)	o	sp	14·03	74·8	5·33	2
DC0315	Perido Pk (Brit. Col.)	o	sp	15·70	72·2	4·60	2
DC0324	Perido Pk (Brit. Col.)	o	sp	8·79	36·2	4·12	2
DC0325	Perido Pk (Brit. Col.)	o	sp	14·35	71·4	4·98	2
GS01-141	Atlin (Brit. Col.)	o	sp	10·69	50·4	4·71	2
GS01-144	Atlin (Brit. Col.)	o	sp	11·69	59·1	5·06	2
GS01-033	Cascaden Ridge (AK)	o	sp	9·96	34·2	3·43	2
GS01-037	Cascaden Ridge (AK)	o	sp	10·46	35·5	3·39	2
GS01-040	Cascaden Ridge (AK)	o	sp	10·34	33·0	3·19	2
GS01-048	American Creek (AK)	o	sp	11·81	47·3	4·01	2
GS01-050	American Creek (AK)	o	sp	8·47	32·8	3·88	2
GS01-058	American Creek (AK)	o	sp	11·70	48·0	4·10	2
GS01-066	American Creek (AK)	o	sp	11·05	40·5	3·67	2
GS01-067	American Creek (AK)	o	sp	9·92	38·1	3·84	2
GS01-068	American Creek (AK)	o	sp	11·04	38·3	3·47	2
GS01-071	American Creek (AK)	o	sp	9·82	35·9	3·66	2
GS01-105	Atlin (Brit. Col.)	o	sp	3·93	7·0	1·79	2
GS01-110	Atlin (Brit. Col.)	o	sp	10·38	34·9	3·36	2
GS01-114	Atlin (Brit. Col.)	o	sp	9·65	39·4	4·08	2
GS01-124	Atlin (Brit. Col.)	o	sp	8·01	30·2	3·76	2
GS01-125	Atlin (Brit. Col.)	o	sp	10·50	37·4	3·56	2
GS01-126	Nahlin Mtn (Brit. Col.)	o	sp	13·13	57·0	4·34	2
GS01-136	Atlin (Brit. Col.)	o	sp	7·18	24·5	3·42	2
GS01-001	Pinchi Lake (Brit. Col.)	o	sp	9·06	21·4	2·36	2
GS01-003	Pinchi Lake (Brit. Col.)	o	sp	7·88	24·9	3·15	2

Sample name	Sample locality	Class	Rock type	Sc	V	V/Sc	Analyst*
DC00·12	Lake Laberge (Yukon)	o	sp	15·39	58·4	3·80	2
DC00·13	Lake Laberge (Yukon)	o	sp	8·61	39·4	4·57	2
BPP008	Buffalo Pitts (Yukon)	om	sp	16·75	68·6	4·10	2
KE001	Buffalo Pitts (Yukon)	om	sp	14·54	65·4	4·50	2
KE003	Buffalo Pitts (Yukon)	om	Sp	13·11	74·1	5·65	2
BPP009	Buffalo Pitts (Yukon)	om	Sp	14·17	60·5	4·27	2
DC00·04	Buffalo Pitts (Yukon)	om	Sp	13·93	68·1	4·89	2
DC00·5	Buffalo Pitts (Yukon)	om	Sp	13·23	74·3	5·62	2

x, xenolith; o, ophiolite; om, orogenic massif; sp, spinel peridotite; sp–gt, garnet-bearing spinel peridotite; serp, partially serpentinized peridotite; AK, Alaska; Brit. Col., British Columbia. *1, Rice University; 2, University of Victoria; 3, Australia National University.

Table A2: Cascades arc magmas

	Mount Shasta, CA											
	95–15		82–72a		85–38a		85–44		82–94a		85–41b	
Analyst:	1	4	1	5	1	4	1	4	1	4	1	4
SiO_2 (wt %)		50·93		47·60		49·14		51·18		52·50		57·87
TiO_2 (wt %)		0·66		0·59		0·87		0·59		0·72		0·60
Al_2O_3 (wt %)		15·54		18·50		16·95		15·84		15·30		14·67
FeO* (wt %)		7·36		8·18		8·62		7·83		7·07		5·69
MnO (wt %)		0·14		0·15		0·18		0·16		0·14		0·11
MgO (wt %)		10·65		10·50		9·60		10·65		10·17		8·88
CaO (wt %)		9·94		12·00		10·61		9·65		9·61		8·13
Na_2O (wt %)		2·73		2·26		2·11		2·21		3·01		3·18
K_2O (wt %)		0·76		0·07		0·30		0·41		0·58		0·72
P_2O_5 (wt %)		0·28		0·06		0·11		0·11		0·22		0·16
Mg-number		0·72		0·70		0·67		0·71		0·72		0·74
Sc (ppm)	33·2	32·0	40·8	31·8	40·0	40·0	35·4	33·0	33·0	31·0	24·6	
V (ppm)	229	219	221	178	221	229	236	226	238	234	172	
Ba (ppm)	397	347	28	17	137	136	125	127	284	262	191	189
La (ppm)	16·5	16·2	1·8	1·3	5·1	5·2	4·2	4·2	12·1	11·4	11·1	10·7
Ce (ppm)	39·1	34·6	5·3	3·8	12·4	11·5	10·0	9·2	24·3	25·8	23·7	24·2
Pr (ppm)	4·85	4·61	0·84		1·76	1·79	1·42	1·43	3·33	3·42	3·13	3·33
Nd (ppm)	20·3	19·3	4·7	3·6	8·8	8·3	7·0	6·5	14·6	14·1	13·0	12·9
Sm (ppm)	3·78	3·80	1·73	1·34	2·66	2·57	1·99	1·91	3·13	3·01	2·60	2·60
Eu (ppm)	1·26	1·08	0·77	0·62	1·06	0·97	0·77	0·69	1·11	0·93	0·91	0·85
Gd (ppm)	4·01	3·13	2·02	1·96	2·94	3·35	2·13	2·32	3·42	2·91	2·83	2·42
Tb (ppm)	0·57		0·37		0·51	0·60	0·35	0·39	0·50	0·44	0·41	0·35
Dy (ppm)	3·10	2·79	2·69	2·66	3·47	3·83	2·22	2·44	2·81	2·48	2·19	1·94
Ho (ppm)	0·55		0·75		0·91	0·88	0·55	0·53	0·55	0·51	0·40	0·40
Er (ppm)	1·60	1·67	2·32	1·76	2·74	2·41	1·65	1·46	1·62	1·38	1·15	1·07
Tm (ppm)	0·24		0·35		0·42	0·39	0·25	0·24	0·24	0·22	0·17	0·16
Yb (ppm)	1·48	1·63	2·70	1·70	2·48	2·60	1·48	1·57	1·46	1·43	1·04	1·05
Ba/Yb	268	213	10	10	55	52	84	81	195	183	183	180
V/Sc	6·89	6·84	5·42	5·60	5·53	5·73	6·67	6·85	7·21	7·55	6·97	

Table A2: continued

	Southern Washington				
	L01-3b	L01-6	L01-17	L01-24	L00-8
Analyst:	1	1	1	1	1
SiO_2 (wt %)	50·66	49·64	51·82	51·55	49·62
TiO_2 (wt %)	1·24	1·14	1·76	1·42	2·00
Al_2O_3 (wt %)	15·82	17·0	16·93	16·76	16·58
FeO* (wt %)	7·90	8·74	9·15	8·95	9·06
MnO (wt %)	0·13	0·15	0·14	0·15	0·15
MgO (wt %)	8·46	9·43	6·57	7·54	7·90
CaO (wt %)	9·84	9·87	8·39	8·99	9·35
Na_2O (wt %)	3·30	2·95	3·87	3·49	3·40
K_2O (wt %)	2·11	0·82	1·00	0·84	1·40
P_2O_5 (wt %)	0·54	0·22	0·36	0·31	0·55
Mg-number	0·66	0·66	0·56	0·60	0·61
Sc (ppm)	25·2	29·9	27·1	33·1	29·5
V (ppm)	216	229	225	223	252
Ba (ppm)	831	396	284	273	420
La (ppm)	50·9	19·4	18·0	19·8	28·4
Ce (ppm)	123·9	47·0	36·5	46·4	65·4
Pr (ppm)	14·83	6·41	5·00	5·87	8·28
Nd (ppm)	59·8	27·9	23·0	25·4	35·5
Sm (ppm)	10·28	5·35	5·48	5·27	7·10
Eu (ppm)	3·15	1·81	1·93	1·79	2·44
Gd (ppm)	11·95	5·90	6·01	5·66	7·77
Tb (ppm)	1·56	0·84	0·90	0·85	1·10
Dy (ppm)	7·06	4·45	4·93	4·62	5·59
Ho (ppm)	0·80	0·77	0·92	0·89	0·88
Er (ppm)	2·07	2·18	2·50	2·50	2·35
Tm (ppm)	0·29	0·32	0·35	0·37	0·33
Yb (ppm)	1·99	1·99	2·22	2·22	2·07
Ba/Yb	418	199	128	123	203
V/Sc	8·57	7·64	8·31	6·74	8·54

Analyst: 1, Rice University; 4, Grove *et al*. (2002); 5, Bacon *et al*. (1994).